内蒙古西乌珠穆沁旗晚二叠世花岗岩的锆石 U-Pb 年龄、地球化学特征及其构造意义

范玉须¹⁾,李廷栋¹⁾,肖庆辉¹⁾,程杨²⁾,李岩²⁾,郭灵俊³⁾,罗鹏跃³⁾ 1)中国地质科学院地质研究所,北京,100037;

2) 中国冶金地质总局矿产资源研究院,北京,101300;3) 内蒙古自治区地质调查院,呼和浩特,010020

内容提要: 西乌珠穆沁旗西南部色尔崩岩体和努和亭沙拉岩体的锆石 U-Pb 年龄为 255.3±1.4 Ma 和 254.4±3.4 Ma,是晚二叠世晚期岩浆活动的产物。岩石地球化学分析发现,花岗岩属于钙碱系列,富钠贫钾,具有高 Sr(Sr \geq 741×10⁻⁶)低 Y、Yb 及高 Sr/Y 的特点,轻重稀土分异显著 (10.25<(La/Yb) $_{\rm N}$ <22.51),弱的正 Eu 异常 (1.06< δ Eu<1.46),富集大离子亲石元素 (LILE),亏损高场强元素 (HFSE),与典型的高锶低钇中酸性岩 (adakite,亦有人译为埃达克岩)地球化学特征相似。岩浆锆石具有正的 $\varepsilon_{\rm Hf}(t)$ 值 (+8.1~+13.3) 和年轻的二阶段模式年龄 ($T_{\rm 2DM}$ 约为 430~760 Ma),高 Mg*(55~59),表明岩浆熔体与地幔橄榄岩发生了相互作用,暗示这种高锶低钇型花岗岩的形成与俯冲板片在深部发生部分熔融有关。结合区域地质资料认为,古亚洲洋在晚二叠世还未完全闭合,研究区内高锶低钇型花岗岩形成于古亚洲洋持续向北俯冲且俯冲洋壳断离并发生部分熔融构造背景下。

关键词:晚二叠世;高锶低钇花岗岩;锆石 U-Pb 定年;古亚洲洋;构造环境

中亚造山带是全球最大的增生型造山带及大陆 地壳牛长最显著的地区。长期以来,关于该造山带 的构造分区及演化、大陆地壳的增生以及矿产资源 形成和分布规律的研究一直是国内外学者关注和研 究的热点(Sengör et al., 1993; Xiao Wenjiao et al., 2003,2009; 肖文交等, 2008; 李锦轶等, 2009; Jian Ping et al., 2010; 汪相, 2018; 吕洪波等, 2018)。但 是,目前不同学者对古亚洲洋最终闭合消失的位置 和时间仍存在不同的认识,主要有两种观点:一种观 点认为古亚洲洋在早古生代已经闭合,晚古生代处 于伸展拉张环境 (Xu Bei and Chen Bin, 1993;徐备 等, 2014));另一种观点认为古亚洲洋俯冲一直持 续到晚古生代至早中生代(Xiao Wenjiao et al., 2003:李锦轶等, 2007)。持后一种观点的学者对古 亚洲洋最终闭合的位置存在3种不同的认识:①沿 索伦—贺根山蛇绿岩带闭合(Cao Congzhou et al., 1986);②沿索伦—林西蛇绿岩带闭合(王荃 1986, 1991; Xiao Wenjiao et al., 2003)); ③中晚三叠世沿 索伦—西拉木伦—延吉蛇绿岩带闭合碰撞(王玉 净,1997;孙德友等,2004;李锦轶等,2007)。最近,

一些新的观点认为古亚洲洋闭合时间可能为早二叠世(汪相,2018),甚至闭合时间可以推迟到晚白垩世(吕洪波等,2018)。因此,晚古生代作为构造体制转换的重要阶段,对这一阶段构造—岩浆演化的研究,有助于正确理解和认识古亚洲洋构造域的增生造山过程以及年轻大陆地壳的生长机制等问题。

高锶低钇型中酸性岩(Adakite,亦有人音译为 埃达克岩)是与岛弧作用有关的、具有独特地球化 学特征的中酸性岩石,是俯冲消减带中俯冲板片熔 融的产物(Defant and Drummond, 1990;许继峰等, 2014),利用高锶低钇型中酸性岩可以追踪地质历 史上的洋壳俯冲及地壳增厚等相关事件,对反演下 地壳组成及成矿作用具有重要意义。目前,在中亚 造山带东南段已经识别出了许多高锶低钇型中酸性 岩岩体,形成时代主要有3个阶段:①早古生代高 锶低钇型中酸性岩,主要分布在内蒙古中部的华北 板块北缘,代表古亚洲洋早期的俯冲作用(许立权 等,2003;刘敦一等,2003;秦亚等,2013);②二 叠纪高锶低钇型中酸性岩,主要分布在二连一贺根 山构造带(张玉清,2009;王金芳等,2017);③三叠

注: 本文为内蒙古自治区地质矿产勘查基金资助项目(编号:2017-YS01)和中国地质调查项目(编号:DD20160345)的成果。

收稿日期:2018-06-13;改回日期:2018-10-13;责任编辑:章雨旭。Doi: 10.16509/j.georeview.2019.01.017

作者简介:范玉须,男,1987年生,博士研究生,构造地质学专业。Email:562442919@qq.com。通讯作者:肖庆辉,男,1939年生,博士生导师,主要从事花岗岩大地构造学,矿产资源成矿地质背景研究,Email:qinghuixiao@126.com。

纪高锶低钇型中酸性岩,主要分布在林西地区(王冬兵等,2009;刘建峰等,2014)。本文研究的高锶低钇型中酸性岩位于贺根山构造带与锡林浩特—达青牧场蛇绿岩带之间,前人研究认为是侏罗纪后造山期的岩浆岩,但是缺少精确的同位素年龄数据[●]。本文通过详细的岩石学、地球化学、锆石 U-Pb 年代学和锆石的 Lu-Hf 同位素研究,结合区域上同时代岩石构造组合,探讨了其岩石成因及其对中亚造山

带东南部晚二叠世的构造演化的指示意义。

1 地质背景

研究区位于中亚造山带东南缘,华北克拉通的北缘,古生代时期经历了古亚洲洋多阶段俯冲、地壳增生和多地体聚合,是古生代俯冲增生造山带(图 1 a;李双林和欧阳自远 1998; Xiao Wenjiao et al., 2003; Windey et al., 2007)。区内古生代的地层主要

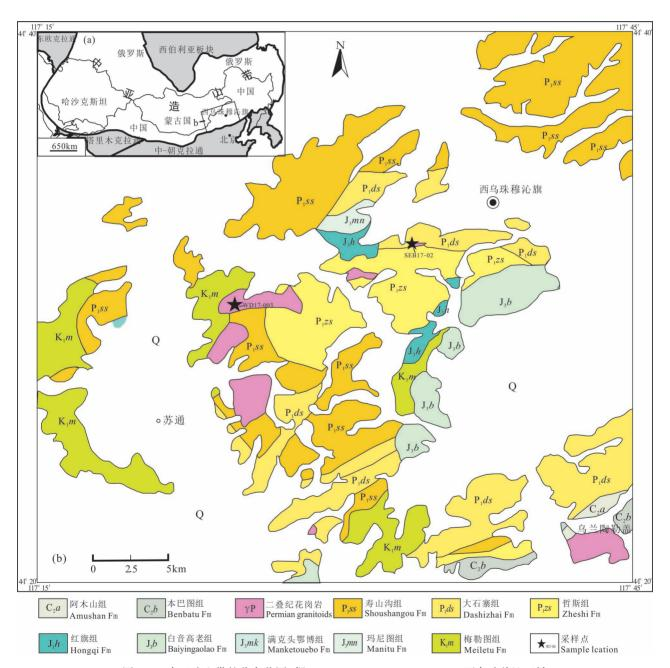


图 1 (a)中亚造山带的分布范围(据 Liu Jianfeng et al., 2016);(b)西乌珠穆沁区域 地质简图(据 1:25 万西乌珠穆沁旗幅修改)

Fig. 1 (a) Distribution range of the Central Asian Orogenic Belt (modified from Liu Jianfeng et al., 2016); (b) simplified geological map of West Ujimqin area, Inner Mongolia (based on 1: 250000 Regional Geological Map)

为二叠纪寿山沟组、大石寨组和 哲斯组,其次为石炭纪阿木山组和本巴图组。晚二叠世至三叠纪地层缺失,部分地区被中生代的火山岩覆盖(图 1b)。研究区内侵入岩较少,努和亭沙拉岩体分布在西乌旗西南 15 km 的温多尔乌拉东南部一带,共有两个侵入体,总面积 10 km²。岩体侵入到中二叠统哲斯组中,下白垩统梅勒图组不整合与其上,岩体呈椭圆状、长轴东西向展布。色尔崩花岗斑岩呈不规则岩株、岩脉侵入到哲斯组生物碎屑灰岩中。

2 岩石特征

样品 WD17-003 采自努和亭沙拉岩体,采样位置为:N44°30′04";E117°25′10"。岩石为中细粒花岗斑岩,灰绿—灰褐色,斑状结构。斑晶为斜长石、钾长石及黑云母。斜长石:半自形、自形,板状,具卡氏双晶和聚片双晶,普遍绢云母化,粒径 0.3~1.2 mm,含量约占整个岩石总量的 15%~20%。钾长石:自形板状,卡氏双晶亦已绢云母化,粒径 0.3~1.2 mm,含量约占岩石总量的 2%。角闪石:长柱

状,横切面六边形几乎全部蚀变,仅呈角闪石假像,蚀变产物为黑云母、绿泥石及铁质,一部分晶体碎裂。粒径 0.2~1.3 mm,多数 0.6~0.8 mm,含量约占岩石总量的 2%。基质由微粒长石、石英及暗色矿物组成。粒径 0.03~0.05 mm,基质占岩石总量的 65%~80%。

2019年

样品 SEB17-002 采自色尔崩花岗岩体,采样位置为:N44°31′57";E117°34′00"。色尔崩花岗斑岩呈灰绿色,斑状结构(图 2),块状构造。斜长石(25%~30%)为主,含少量暗色矿物,杂乱分布,局部见聚斑或联斑产出,粒径 0.2~5.5 mm,斜长石多呈半自形板状、宽板状、板条状,部分边缘熔蚀,聚片双晶发育,双晶较宽;暗色矿物已蚀变,被绿泥石、褐铁矿、少量碳酸盐交代。基质由长英质(65%~70%)和少量暗色矿物组成,为粒径<0.2 mm 的微晶、细晶,见少量微晶板条状斜长石。

3 分析方法

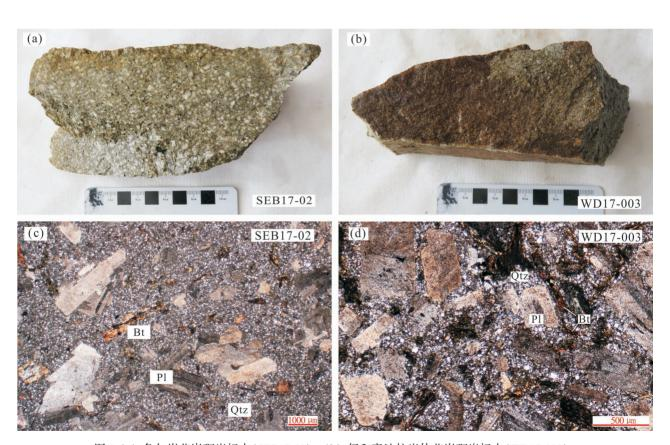


图 2 (a) 色尔崩花岗斑岩标本(SEB17-02); (b) 努和亭沙拉岩体花岗斑岩标本(WD17-003); (c) 色尔崩花岗斑岩镜下照片; (d) 努和亭沙拉花岗斑岩镜下照片

Fig. 2 (a) The sample of the Seerbeng granite-porphyry (SEB17-02); (b) the Nuhetingshala granite-porphyry from (WD17-003); (c) microphoto of the Seerbeng granite-porphyry; (d) microphoto of the Nuhetingshala granite-porphyry

3.1 岩石主微量元素分析

全岩的主量元素分析在南京大学内生金属矿床成矿机制研究国家重点实验室完成。将制备好的碱熔玻璃片在 ARL 9900 型 X 射线荧光光谱仪(XRF)上进行分析测试。碱熔玻璃片的制备过程为:将1g粉末样品与11g助熔剂充分混合后倒入铂金坩埚,通过 THEOXD 全自动电熔融炉进行熔融,制备成玻璃片。样品分析测试的电流和电压分别为75mA和40kV。样品浓度>1.0%时分析相对误差在±1%;当样品浓度<1.0%时,相对误差则在±10%。微量元素和稀土元素用ICP-MS 法测定,仪器型号为ELEMENT-2质谱仪,相对误差约2%。

3.2 锆石 LA-ICP-MS U-Pb 定年

锆石分选是在廊坊诚信地质服务公司完成,锆石 CL 图像拍摄和制靶在北京锆年领航公司完成。锆石 U-Pb 同位素定年在中国地质大学(北京)科学研究院实验中心完成,实验方法为 LA-ICP-MS 微区原位定年,实验仪器为 193 nm 准分子激光器和电感

耦合等离子质谱仪(型号 Thermo Xseries2)。实验中激光的束斑直径为 32 μm,频率为 6 Hz,以 He 气作为 载 气。数 据 处 理 和 谐 和 图 绘 制 采 用 ICPMSDataCal(Liu Yongsheng et al., 2010)和 Isoplot 3.0 程序获得。

3.3 锆石 Hf 同位素

告石 Hf 同位素的分析是在锆石 U-Pb 同位素分析基础上完成的,测试在中国地质科学院地质研究所大陆构造与动力学实验室完成,使用仪器为 Neptune Plus 型多接收等离子质谱和 Geo Las Pro193nm 激光剥蚀系统 (LA-MC-ICP-MS),实验过程中采用 He 作为剥蚀物质载气,根据锆石大小,激光剥蚀系统直径采用 44 μ m,测定时使用锆石国际标样 GJ-1 作为参考物质。相关仪器运行条件及详细分析流程见侯可军等(2007)。分析过程中锆石标准 GJ-1 的 $n(^{176}$ Hf)/ $n(^{177}$ Hf)测试加权平均值分别为 0.282008 ± 0.000050 (2 σ)。计算 初始 $n(^{176}$ Hf)/ $n(^{177}$ Hf)时,Lu 的衰变常数采用 1.865×

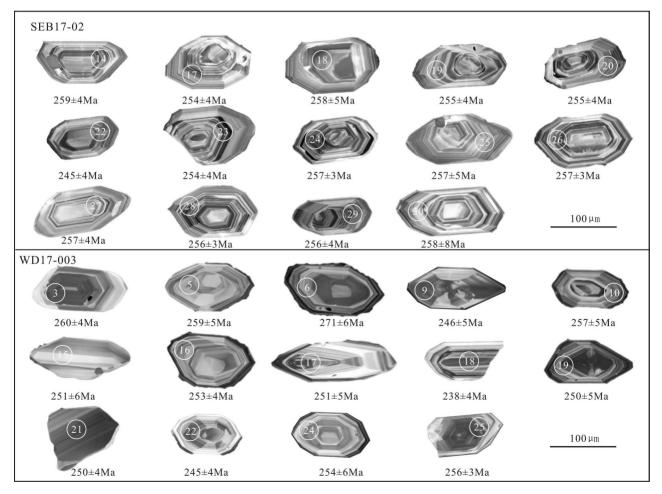


图 3 高锶低钇花岗岩中部分锆石阴极发光图像

Fig. 3 Cathodoluminescence (CL) images showing internal textures of zircons from granitoid

 10^{-11} a⁻¹(Scherer et al., 2001), $\varepsilon_{\rm Hf}(t)$ 值的计算采用 球粒 陨石 Hf 同位素值 $n (^{176}$ Lu $)/n (^{177}$ Hf $) = 0.0332, <math>n (^{176}$ Hf $)/n (^{177}$ Hf) = 0.282772 (Blichert – Toft et al., 1997)。

4 分析结果

4.1 锆石 U-Pb 定年结果

锆石 U-Pb 定年结果见表 1。

色尔崩花岗斑岩(SEB17-02) 锆石晶型较好,粒径大于 $100~\mu m$,呈棱柱状,CL 图像中可见清晰的震荡环带(图 3),Th/U 为 $0.45\sim1.24$,平均值为 0.91,远大于 0.4(表 1),显示了典型岩浆锆石特征。样品(SEB17-02)共获得 27~个有效测点,锆石年龄协和一致,基本都位于谐和线附近(图 4a),说明锆石形成后没有 Pb 的丢失,测年数据具有较高的可信度,其 $^{206}Pb/^{238}$ U 的加权平均年龄值为 255.3 ± 1.4

Ma(MSDW=0.65)(图 4b),代表了岩体冷凝侵位的 年龄。

努和亭沙拉花岗斑岩中锆石呈棱柱状,CL图像显示具有震荡环带(图3),Th/U为0.35~1.11,平均为0.62,为岩浆结晶锆石成因。本次获得21个有效测点,年龄谐和度较高,集中在谐和线附件(图4c),表明锆石没有受到后期构造热事件影响而发生Pb的丢失,努和亭沙拉花岗斑岩(WD17-03)的锆石²⁰⁶Pb/²³⁸U年龄的加权平均值为254.4+3.4 Ma(MSDW=1.9)(图4d),属于晚二叠世晚期,代表了努和亭沙拉岩体的冷凝侵位的年龄。

4.2 主微量元素分析结果

花岗岩的主微量元素分析结果见表 2,其中烧失量(LOI)为 1.53%~3.54%,说明岩石可能受到后期蚀变的影响,投图时扣除烧失量归一化后重新计算氧化物含量。由表中可以看出,努和亭沙拉花岗

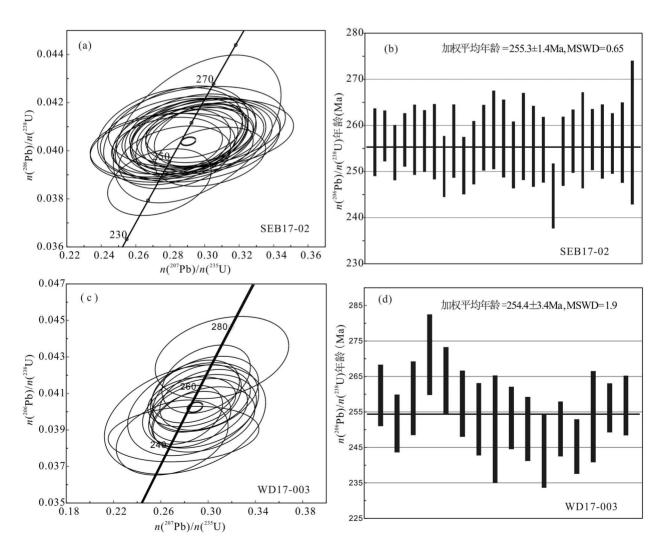


图 4 锆石 U-Pb 年龄谐和图及加权平均年龄

Fig. 4 Zircon U-Pb Concordia diagrams of the granites from the West Ujimqin area

表 1 西乌珠穆沁旗晚二叠世高锶低钇型花岗岩的锆石 U-Pb 同位素微区原位分析结果 Table1 LA-ICP-MS data of zircons from Late Permian adakitic granite in West Ujimqin area

1995年 1995		元素	元素含量(×10-6)	(9_0				同位素比值	ぎ比値					同位素年龄(Ma	龄(Ma)			
70 70 30 30 10 30 10 30 10 30 10 30 10 30 10 30 10 30 10 30 10 30 10 30 10 30 10 30 10 30	测点号	Ē	Ē	Ė	Th/U	n(²⁰⁷ Pb)/	/n(²⁰⁶ Pb)	$n(^{207}\mathrm{Pb})$	/n(²³⁵ U)	$n(^{206}\mathrm{Pb})$	$/n(^{238}{ m U})$	$n(^{207}\mathrm{Pb})/i$	n(206Pb)	$n(^{207}\mathrm{Pb})$ /	n(235U)	$n(^{206}\text{Pb})/n(^{238}\text{U})$	$n(^{238}\mathrm{U})$	谐和度
19.05 19.02 19.05 19		Z Q	uI	<u> </u>		测值	1σ	测值	1σ	测值	1σ	测值	1σ	测值	1σ	测值	1σ	(%)
9.088 100.2 176.6 6.8672 0.0823 0.0029 0.0148 0.0040 4.30.6 4.31.4 118.5 2.88.7 11.5 2.5.63 3.31.8 4.30.2 1.023.2 0.0022 0.0232 0.0022 0.0290 0.0118 0.0004 30.6 9.7 2.6.7 11.5 3.35. 1.30.7 2.6.1 10.0 2.8.2 1.0.2 0.0023 0.0029 0.0297 0.0000 3.44.5 11.2 10.3 2.6.1 10.0 1.2.7 2.44.3 2.44.1 0.9133 0.0623 0.0027 0.2994 0.0407 0.0006 2.88.2 11.2 10.3 10.0 2.89.2 10.0 2.89.2 10.0 2.89.2 10.0 2.89.2 10.0 2.89.2 10.0 2.89.2 10.0 2.89.2 10.0 2.89.2 10.0 2.89.2 10.0 2.89.2 0.0 2.89.2 10.0 2.89.2 0.0 2.89.2 0.0 2.89.2 10.0 2.89.2 0.0 2.89.2						样品号		, 采自色尔	崩花岗岩体	,采样位置为	1: N44°31′57	7"; E117°34'	,00					
2.5.63 53.1.8 49.0.5 1.23.5 0.052.5 0.0021 0.2940 0.0115 0.0000 30.56 90.7 26.1.7 9.00 17.26 333.2 339.2 0.0823 0.0023 0.2781 0.0122 0.0407 0.0005 211.2 10.2 26.1.7 9.03 17.27 334.2 399.2 0.0823 0.0023 0.0273 0.017 0.0407 0.0005 344.5 11.94 264.1 11.0 17.24 17.6.7 23.3.2 0.6879 0.0524 0.0027 0.2906 0.0140 0.0000 344.5 11.94 264.1 11.0 1.3.2 17.6.7 23.3.4 0.6879 0.0224 0.0027 0.2940 0.0196 0.0000 344.5 11.24 11.24 11.24 11.24 11.24 11.24 11.24 11.24 11.24 11.24 11.24 11.24 11.24 11.24 11.24 11.24 11.24 11.24 12.24 11.24 12.24 12.2	SEB17-02-1	9.085	100.2	176.6	0.5672	0.0553	0.0029	0.3030	0.0148	0.0406	9000.0	433.4	118.5	268.7	11.5	256.3	3.7	95
17.26 333.2 365.1 1092 0.0801 0.023 0.0407 0.0407 0.0006 344.2 10.2 0.0531 0.0231 0.0231 0.0232 0.0234 0.0232 0.0232 0.0232 0.0331 0.0034 0.0332 0.0340 0.0340 0.0340 0.0343 0.0407	SEB17-02-2	25.63	531.8	430.5	1.235	0.0525	0.0021	0.2940	0.0115	0.0408	0.0004	305.6	7.06	261.7	9.03	257.7	2.8	86
19.57 35.6.2 359.2 0.9082 0.0533 0.0024 0.2971 0.0128 0.0407 0.0005 344.5 103.7 254.1 10.0 10.0 11.2	SEB17-02-3	17.26	333.2	305.1	1.092	0.0501	0.0023	0.2781	0.0132	0.0402	0.0005	211.2	102.8	249.2	10.5	254.1	3.0	86
1.1.2.74 24.43 23.41 0.9153 0.0023 0.0027 0.02973 0.0156 0.04040 0.0006 298.2 1120 2.58.8 10.7 11.2 2.5.3 2.5.4	SEB17-02-4	19.57	326.2	359.2	0.9082	0.0531	0.0024	0.2971	0.0128	0.0407	0.0005	344.5	103.7	264.1	10.0	256.9	2.9	26
13.32 176.7 253.2 0.6879 0.0632 0.0274 0.0294 0.0151 0.0406 0.0000 344.5 119.4 264.4 11.8 9.5.78 11.74 183.2 0.634 0.0524 0.0294 0.0186 0.0000 346.4 112.0 266.2 11.8 16.51 220.4 0.034 0.0024 0.0296 0.0176 0.0000 346.4 112.0 267.2 11.8 16.15 222.9 283.9 0.0949 0.0329 0.0076 0.0196 0.0000 346.4 112.4 267.1 11.7 16.15 282.9 0.0894 0.0023 0.0130 0.0196 0.0000 346.4 11.2 267.1 11.7 16.11 282.9 0.0894 0.0032 0.0132 0.0132 0.0040 0.0040 0.0000 346.4 11.2 267.1 11.7 16.11 27.2 0.0023 0.0234 0.0132 0.0132 0.0249 0.0249 0.0249	SEB17-02-5	12.74	214.3	234.1	0.9153	0.0523	0.0027	0.2903	0.0136	0.0407	9000.0	298.2	112.0	258.8	10.7	256.9	3.8	66
9.578 117.4 185.2 0.634 0.0524 0.0234 0.0150 0.0406 0.0007 301.9 112.0 287.1 117.4 14.40 2.92.4 303.4 0.0571 0.0524 0.0224 0.228.2 0.0131 0.0000 346.4 112.0 282.7 10.0 14.40 2.82.9 3.83.4 0.0549 0.0532 0.0023 0.0131 0.0000 433.4 92.6 112.0 282.7 10.0 16.61 2.82.9 0.8916 0.0534 0.0023 0.0132 0.0000 187.1 132.4 92.7 10.0 16.01 2.82.9 3.83.6 0.0949 0.0023 0.0172 0.0407 0.0006 187.1 132.0 187.1 13.7 13.7 13.8 13.8 13.8 18.8 0.0024 0.0259 0.0219 0.0407 0.0006 18.7 19.0 0.0249 0.0259 0.0210 0.0407 0.0006 18.3 1.3 18.7 18.7 18.7	SEB17-02-6	13.32	176.7	253.2	0.6979	0.0532	0.0027	0.2975	0.0151	0.0406	0.0005	344.5	119.4	264.4	11.8	256.6	3.3	26
14.31 290.4 303.4 0.0571 0.0234 0.0326 0.0133 0.0396 0.0006 346.4 112.0 252.7 10.5 14.40 282.2 287.3 0.9049 0.0034 0.0309 0.0176 0.0406 0.0006 346.4 112.4 287.1 13.7 16.01 282.2 287.3 0.9049 0.0036 0.0309 0.0135 0.0105 0.0006 343.4 97.2 288.9 10.048 0.036 0.3049 0.0135 0.0006 187.1 15.0 287.1 13.7 11.6.0 277.2 1.049 0.0498 0.0303 0.035 0.0407 0.0006 39.4 15.0 287.1 13.7 11.4.1 234.4 238.1 0.0349 0.0239 0.0135 0.0407 0.0007 39.3 119.4 13.7 13.7 11.4.1 234.4 238.1 0.0359 0.0229 0.0135 0.0401 0.0007 39.3 119.4 15.2 15.2	SEB17-02-7	9.578	117.4	185.2	0.634	0.0524	0.0027	0.2934	0.0150	0.0406	0.0007	301.9	112.0	261.2	11.7	256.5	4.1	86
14.40 232.9 287.3 0.9049 0.0534 0.0300 0.3000 0.0176 0.0006 346.4 132.4 267.1 13.7 16.15 282.9 283.9 0.0964 0.0553 0.0023 0.3032 0.0131 0.0906 433.4 97.2 268.9 10.2 16.01 282.9 283.9 0.0964 0.0584 0.0032 0.2356 0.0197 0.0000 187.1 150.0 269.9 150.0 187.1 150.0 269.9 180.0	SEB17-02-8	16.31	290.4	303.4	0.9571	0.0518	0.0024	0.2826	0.0133	0.0397	0.0005	276.0	112.0	252.7	10.5	251.1	3.3	66
16.15 28.29 28.3.9 0.9964 0.0553 0.0023 0.2356 0.0131 0.0398 0.0005 433.4 97.2 26.89 10.2 11.108 117.4 199.0 0.8946 0.0038 0.0325 0.0175 0.0409 0.0006 0.0340 0.0175 0.0409 0.0009 0.2256 0.0175 0.0407 0.0006 390.8 150.0 247.1 13.7 14.11 23.4.4 238.1 0.0847 0.0036 0.2956 0.0156 0.0407 0.0007 390.8 119.8 150.0 247.1 13.7 14.54 244.9 238.9 0.0524 0.0229 0.2996 0.0156 0.0494 0.0209 0.2996 0.0496 0.0409 0.0209 0.2996 0.0172 0.0409 0.0009 0.2299 0.0409 0.0409 0.0209 0.0212 0.0409 0.0009 0.0212 0.0409 0.0009 0.0409 0.0009 0.0409 0.0009 0.0409 0.0409 0.0009 <td< td=""><td>SEB17-02-9</td><td>14.40</td><td>232.9</td><td>257.3</td><td>0.9049</td><td>0.0534</td><td>0.0030</td><td>0.3009</td><td>0.0176</td><td>0.0406</td><td>9000.0</td><td>346.4</td><td>132.4</td><td>267.1</td><td>13.7</td><td>256.6</td><td>4.0</td><td>96</td></td<>	SEB17-02-9	14.40	232.9	257.3	0.9049	0.0534	0.0030	0.3009	0.0176	0.0406	9000.0	346.4	132.4	267.1	13.7	256.6	4.0	96
11.08 17.74 199.0 0.8916 0.04948 0.0035 0.02755 0.0402 0.0006 187.1 150.0 247.1 13.7 16.01 277.9 264.9 1.049 0.05344 0.0034 0.0295 0.0407 0.0006 390.8 150.0 269.5 15.2 14.11 234.4 238.1 0.0847 0.0534 0.0295 0.0210 0.0401 0.0007 344.5 16.9 269.9 15.2 14.54 244.9 0.539 0.0525 0.0201 0.0401 0.0007 390.8 16.8 15.2 14.54 244.9 0.539 0.0526 0.0201 0.0403 0.0401 0.0007 16.8 16.8 15.2 14.54 244.9 0.0529 0.0202 0.0403 0.0403 0.0403 0.0403 0.0403 0.0403 0.0403 0.0403 0.0403 0.0403 0.0403 0.0403 0.0403 0.0403 0.0403 0.0403 0.0403 0.0403 0	SEB17-02-10	16.15	282.9	283.9	0.9964	0.0553	0.0023	0.3032	0.0131	0.0398	0.0005	433.4	97.2	268.9	10.2	251.3	3.1	93
16.01 277.9 264.9 1.049 0.0544 0.0364 0.3040 0.0195 0.0407 0.0006 390.8 150.0 269.5 15.2 14.11 234.4 238.1 0.9847 0.0525 0.0295 0.2010 0.0401 0.0000 34.5 16.5 26.9 16.5	SEB17-02-11	11.08	177.4	199.0	0.8916	0.0498	0.0032	0.2755	0.0172	0.0402	9000.0	187.1	150.0	247.1	13.7	254.1	3.4	76
14.11 234.4 238.1 0.9847 0.0031 0.0295 0.0210 0.00410 0.0007 344.5 163.9 262.9 16.5 13.87 193.8 247.3 0.7839 0.0255 0.0029 0.2917 0.0135 0.0407 0.0007 399.3 119.4 259.9 10.2 10.32 91.27 202.0 0.4519 0.0259 0.0172 0.0408 0.0009 164.9 164.9 150.9 152.1 10.32 91.27 202.0 0.4519 0.0294 0.0299 0.0172 0.0409 164.9 0.0299 164.9 0.0009 164.9 164.9 164.9 165.9 <td>SEB17-02-12</td> <td>16.01</td> <td>277.9</td> <td>264.9</td> <td>1.049</td> <td>0.0544</td> <td>0.0036</td> <td>0.3040</td> <td>0.0195</td> <td>0.0407</td> <td>9000.0</td> <td>390.8</td> <td>150.0</td> <td>269.5</td> <td>15.2</td> <td>257.3</td> <td>3.6</td> <td>95</td>	SEB17-02-12	16.01	277.9	264.9	1.049	0.0544	0.0036	0.3040	0.0195	0.0407	9000.0	390.8	150.0	269.5	15.2	257.3	3.6	95
13.8 193.8 247.3 0.7839 0.0525 0.0029 0.2917 0.0155 0.0407 0.0007 399.3 119.4 259.9 12.2 14.54 244.9 253.9 0.9647 0.0510 0.0193 0.0401 0.0006 239.0 164.8 251.4 15.3 10.22 91.27 202.0 0.4519 0.0494 0.0029 0.2799 0.0172 0.0404 0.0006 239.0 164.8 251.4 15.3 11.42 160.5 207.7 0.0404 0.0007 0.0404 0.0006 239.0 164.8 251.4 15.3 11.42 160.5 207.7 0.0404 0.0006 0.0404 0.0006 239.0 148.1 250.6 15.6 11.13 200.2 0.0418 0.0212 0.0123 0.0123 0.0123 0.0123 0.0123 0.0124 0.0006 239.0 111.1 251.0 111.1 251.0 111.1 251.0 111.1 251.0 111.1	SEB17-02-13	14.11	234.4	238.1	0.9847	0.0531	0.0039	0.2955	0.0210	0.0410	0.0007	344.5	163.9	262.9	16.5	259.0	4.2	86
14.54 244.9 253.9 0.9647 0.0510 0.0369 0.0193 0.0401 0.0006 239.0 164.8 251.4 15.3 10.32 91.27 202.0 0.4519 0.0494 0.0029 0.2799 0.0172 0.0408 10.000 164.9 130.5 250.6 13.6 11.42 160.5 202.0 0.4519 0.0494 0.0029 0.2199 0.0172 0.0408 0.0000 222.3 148.1 262.6 15.6 11.42 160.5 207.7 0.7724 0.0528 0.0192 0.0193 0.0404 0.0000 229.9 0.0193 0.0403 0.023 0.0193 0.0193 0.0006 229.9 0.0193 0.0019 0.0193 0.0193 0.0006 209.3 111.1 251.9 111.1 251.9 111.1 251.9 111.1 251.9 111.1 251.9 111.1 251.9 111.1 251.9 111.1 251.9 111.1 251.9 111.2 111.2	SEB17-02-14	13.87	193.8	247.3	0.7839	0.0525	0.0029	0.2917	0.0155	0.0407	0.0007	309.3	119.4	259.9	12.2	257.2	4.2	86
10.32 91.27 202.0 0.4519 0.0494 0.0299 0.0172 0.0408 0.6009 160.5 250.0 130.5 250.0 130.2 250.0 130.2 250.0 130.2 1.029 0.0404 0.0404 0.0007 322.3 148.1 262.0 15.6 11.42 160.5 207.7 1.0724 0.0528 0.023 0.2891 0.0121 0.0404 0.0006 279.7 91.6 258.3 9.5 16.86 276.3 320.2 317.7 1.008 0.0510 0.023 0.012 0.012 0.0006 279.7 91.6 285.3 9.5 21.46 416.9 366.8 1.137 0.023 0.023 0.0137 0.0406 0.0006 299.7 10.1 251.0 9.5 20.47 376.3 356.0 1.057 0.0524 0.023 0.0126 0.0126 0.0406 0.0006 279.7 11.1 251.9 13.6 20.47 376.3 188.3	SEB17-02-15	14.54	244.9	253.9	0.9647	0.0510	0.0036	0.2809	0.0193	0.0401	0.0006	239.0	164.8	251.4	15.3	253.6	3.6	66
11.42 160.5 207.7 0.7724 0.0527 0.0934 0.0198 0.0404 0.0000 322.3 148.1 262.6 15.6 18.15 320.2 317.7 1.008 0.0518 0.0121 0.0403 0.0006 279.7 91.6 258.3 9.5 16.86 276.3 317.7 1.008 0.0518 0.023 0.0123 0.0123 0.0006 239.0 11.11 251.9 9.8 21.46 416.9 366.8 1.137 0.0503 0.023 0.0126 0.0406 0.0006 209.3 11.11 251.9 9.8 20.47 376.3 356.0 1.057 0.0524 0.023 0.0126 0.0406 0.0006 227.8 14.4 251.9 9.8 20.47 376.3 0.653 0.0522 0.0126 0.0406 0.0406 0.0006 257.8 13.6 13.6 16.42 383.9 353.6 0.0512 0.021 0.0166 0.0406 0.000	SEB17-02-16	10.32	91.27	202.0	0.4519	0.0494	0.0029	0.2799	0.0172	0.0408	0.0008	164.9	130.5	250.6	13.6	257.6	4.7	26
18.15 320.2 317.7 1.008 0.0518 0.02897 0.0121 0.0403 0.0406 279.7 91.6 258.3 9.5 16.86 276.3 323.4 0.8542 0.0510 0.0023 0.2737 0.0123 0.0387 0.0006 239.0 103.7 245.7 9.8 21.46 416.9 366.8 1.137 0.0524 0.0024 0.2816 0.0126 0.0406 0.0006 239.0 111.1 251.9 10.8 9.9 20.47 376.3 356.0 1.057 0.0524 0.0023 0.0126 0.0406 0.0006 229.3 111.1 251.9 10.8 9.9 8.182 1.68.0 1.657 0.6532 0.0023 0.2834 0.0126 0.0406 0.0006 257.8 144.4 253.3 13.6 1.64.2 330.3 276.7 1.226 0.0512 0.0292 0.0156 0.0406 0.0006 257.8 144.4 253.3 13.6 <t< td=""><td>SEB17-02-17</td><td>11.42</td><td>160.5</td><td>207.7</td><td>0.7724</td><td>0.0527</td><td>0.0034</td><td>0.2951</td><td>0.0198</td><td>0.0404</td><td>0.0007</td><td>322.3</td><td>148.1</td><td>262.6</td><td>15.6</td><td>255.5</td><td>4.4</td><td>26</td></t<>	SEB17-02-17	11.42	160.5	207.7	0.7724	0.0527	0.0034	0.2951	0.0198	0.0404	0.0007	322.3	148.1	262.6	15.6	255.5	4.4	26
16.86 276.3 323.4 0.8542 0.0510 0.0023 0.0123 0.0123 0.0387 0.0006 239.0 103.7 245.7 9.8 21.46 416.9 366.8 1.137 0.0534 0.0024 0.2816 0.0137 0.0406 0.0006 209.3 111.1 251.9 10.8 20.44 416.9 366.8 1.137 0.0524 0.0023 0.2836 0.0126 0.0406 0.0006 201.9 111.1 251.9 10.8 8.182 108.0 155.7 0.6935 0.0524 0.0023 0.2834 0.0126 0.0406 0.0006 227.8 144.4 253.3 13.6 19.21 308.9 353.5 0.8736 0.0528 0.0109 0.0406 0.0005 227.8 144.4 253.3 13.6 10.41 339.3 276.7 1.226 0.0229 0.0286 0.0406 0.0406 0.0005 256.9 12.3 12.3 17.91 331.4	SEB17-02-18	18.15	320.2	317.7	1.008	0.0518	0.0022	0.2897	0.0121	0.0403	0.0006	279.7	91.6	258.3	9.5	254.8	3.6	86
21.46 416.9 366.8 1.137 0.0503 0.0024 0.0137 0.0403 0.0006 209.3 111.1 251.9 10.8 20.47 376.3 356.0 1.057 0.0524 0.0023 0.2939 0.0126 0.0406 0.0006 301.9 100.0 261.6 9.9 8.182 108.0 1.55.7 0.6935 0.0507 0.0032 0.2834 0.0172 0.0406 0.0008 227.8 144.4 253.3 13.6 19.21 308.9 355.5 0.8736 0.0528 0.0019 0.0175 0.0407 0.0008 227.8 144.4 253.3 13.6 10.4.4 308.9 355.5 0.8736 0.0019 0.2876 0.0106 0.0406 0.0005 264.9 12.3 12.3 20.4.1 383.6 351.8 1.000 0.0512 0.0296 0.2956 0.0406 0.0005 264.9 12.3 12.3 17.91 331.4 322.7 1.027	SEB17-02-19	16.86	276.3	323.4	0.8542	0.0510	0.0023	0.2737	0.0123	0.0387	9000.0	239.0	103.7	245.7	8.6	244.7	3.5	66
20.47 376.3 356.0 1.057 0.0524 0.0003 0.2939 0.0126 0.0406 0.0006 301.9 100.0 261.6 9.9 8.182 108.0 155.7 0.6935 0.0507 0.0032 0.2834 0.0172 0.0406 0.0008 227.8 144.4 253.3 13.6 19.21 308.9 353.5 0.8736 0.0528 0.0019 0.2972 0.0108 0.0406 0.0006 255.6 125.9 264.2 8.5 16.42 339.3 276.7 1.226 0.0512 0.0027 0.0156 0.0406 0.0006 255.6 12.3 12.3 17.91 383.6 351.8 1.090 0.0512 0.0291 0.0156 0.0406 0.0005 264.9 91.7 258.6 12.3 17.91 331.4 322.7 1.027 0.0512 0.0296 0.0196 0.0406 0.0013 331.5 149.1 256.6 15.3 1.524 112.8 <	SEB17-02-20	21.46	416.9	366.8	1.137	0.0503	0.0024	0.2816	0.0137	0.0403	9000.0	209.3	1111.1	251.9	10.8	254.4	3.8	66
8.182 108.0 155.7 0.6935 0.0507 0.0032 0.2834 0.0172 0.0406 0.0008 227.8 144.4 253.3 13.6 19.21 308.9 353.5 0.8736 0.0528 0.0019 0.2972 0.0108 0.0407 0.0005 255.6 125.9 264.2 8.5 16.42 339.3 276.7 1.226 0.0512 0.0028 0.2870 0.0156 0.0406 0.0005 255.6 125.9 256.2 12.3 17.91 383.6 351.8 1.090 0.0515 0.0027 0.2901 0.0156 0.0405 0.0005 256.9 17.3 258.6 12.3 17.91 331.4 322.7 1.027 0.0512 0.0039 0.2956 0.0199 0.0409 0.0013 331.5 173.1 256.6 15.3 17.594 112.8 150.2 0.0531 0.0039 0.2956 0.0199 0.0413 331.5 173.1 256.0 15.6	SEB17-02-21	20.47	376.3	356.0	1.057	0.0524	0.0023	0.2939	0.0126	0.0406	0.0006	301.9	100.0	261.6	6.6	256.6	3.4	86
19.21 308.9 353.5 0.8736 0.0528 0.0019 0.2972 0.0108 0.0407 0.0005 320.4 81.5 264.2 8.5 16.42 339.3 276.7 1.226 0.028 0.2870 0.0156 0.0406 0.0006 255.6 125.9 256.2 12.3 20.41 383.6 351.8 1.090 0.0515 0.0024 0.2901 0.0156 0.0406 0.0005 264.9 91.7 258.6 12.3 17.91 331.4 322.7 1.027 0.0512 0.0394 0.2956 0.0199 0.0409 0.0013 331.5 173.1 256.6 15.5 17.594 112.8 150.2 0.7513 0.0531 0.0039 0.2956 0.0199 0.0409 0.0013 331.5 173.1 263.0 15.6 16.08 174.7 309 0.5531 0.0251 0.0256 0.0294 0.0409 0.0013 331.5 112.0 25.1 11.9 <	SEB17-02-22	8.182	108.0	155.7	0.6935	0.0507	0.0032	0.2834	0.0172	0.0406	0.0008	227.8	144.4	253.3	13.6	256.8	5.2	86
16.42 339.3 276.7 1.226 0.0028 0.2870 0.0156 0.0406 0.0006 255.6 125.9 256.2 12.3 20.41 383.6 351.8 1.090 0.0515 0.0027 0.2901 0.0156 0.0405 0.0005 264.9 91.7 258.6 12.3 17.91 331.4 322.7 1.027 0.0512 0.0034 0.2875 0.0196 0.0406 0.0007 250.1 149.1 256.6 15.3 7.594 112.8 150.2 0.7513 0.0531 0.0039 0.2956 0.0199 0.0409 0.0013 331.5 173.1 256.0 15.6 16.08 112.8 150.2 0.7513 0.0531 0.0256 0.0156 0.0446 0.0013 331.5 173.1 263.0 15.6 16.08 174.7 309 0.5654 0.0509 0.0256 0.2894 0.0158 0.0411 0.0007 235.3 112.0 251.4 10.1	SEB17-02-23	19.21	308.9	353.5	0.8736	0.0528	0.0019	0.2972	0.0108	0.0407	0.0005	320.4	81.5	264.2	8.5	256.9	3.3	26
20.41 383.6 351.8 1.090 0.0515 0.0027 0.2901 0.0156 0.0405 0.0005 264.9 91.7 258.6 12.3 17.91 331.4 322.7 1.027 0.0312 0.0034 0.2875 0.0196 0.0406 0.0007 250.1 149.1 256.6 15.5 7.594 112.8 150.2 0.7513 0.0531 0.0034 0.2956 0.0199 0.0409 0.0013 331.5 173.1 256.6 15.6 16.08 174.7 309 0.5654 0.0539 0.0256 0.0152 0.0411 0.0007 235.3 112.0 258.1 11.9 18.74 342.4 347.8 0.9843 0.0517 0.0224 0.0289 0.0128 0.0398 0.0007 333.4 104.6 251.4 10.1	SEB17-02-24	16.42	339.3	276.7	1.226	0.0512	0.0028	0.2870	0.0156	0.0406	0.0006	255.6	125.9	256.2	12.3	256.5	4.0	66
17.91 331.4 322.7 1.027 0.0512 0.034 0.2856 0.0196 0.0406 0.0007 250.1 149.1 256.6 15.5 7.594 112.8 150.2 0.7513 0.0531 0.0039 0.2956 0.0199 0.0409 0.0013 331.5 173.1 263.0 15.6 16.08 112.8 150.2 0.0531 0.0039 0.2956 0.0199 0.0409 0.0013 331.5 173.1 263.0 15.6 16.08 174.7 309 0.5654 0.0509 0.0025 0.2894 0.0128 0.0411 0.0007 235.3 112.0 258.1 11.9 18.74 342.4 342.8 0.9843 0.0517 0.024 0.2809 0.0128 0.0398 0.0007 333.4 104.6 251.4 10.1	SEB17-02-25	20.41	383.6	351.8	1.090	0.0515	0.0027	0.2901	0.0156	0.0405	0.0005	264.9	91.7	258.6	12.3	256.1	3.3	66
7.594 112.8 150.2 0.7513 0.0531 0.0039 0.2956 0.0199 0.0409 0.0013 331.5 173.1 263.0 15.6 16.08 174.7 309 0.5654 0.0509 0.0025 0.2894 0.0152 0.0411 0.0007 235.3 112.0 258.1 11.9 18.74 342.4 347.8 0.9843 0.0517 0.0024 0.2809 0.0128 0.0388 0.0077 333.4 104.6 251.4 10.1	SEB17-02-26	17.91	331.4	322.7	1.027	0.0512	0.0034	0.2875	0.0196	0.0406	0.0007	250.1	149.1	256.6	15.5	256.3	4.4	66
16.08 174.7 309 0.5654 0.0507 0.0024 0.0024 0.0128 0.0128 0.0039 0.0039 0.0128 0.0128 0.0039 0.0039 0.0024 0.0289 0.0128 0.0128 0.0007 333.4 104.6 251.4 10.1	SEB17-02-27	7.594	112.8	150.2	0.7513	0.0531	0.0039	0.2956	0.0199	0.0409	0.0013	331.5	173.1	263.0	15.6	258.4	7.8	86
16.08 174.7 309 0.5654 0.0509 0.0025 0.2894 0.0152 0.0411 0.0007 235.3 112.0 258.1 11.9 18.74 342.4 347.8 0.9843 0.0517 0.0024 0.2809 0.0128 0.0398 0.0007 333.4 104.6 251.4 10.1					样品号:			沙拉岩体,	岩石为中细	粒花岗斑岩	,采样位置。	\$\tau_1.N44°30′()4"; E117°	25'10"				
18.74 342.4 347.8 0.9843 0.0517 0.0024 0.2809 0.0128 0.0398 0.0007 333.4 104.6 251.4 10.1	WD17-003-3	16.08	174.7	309	0.5654	0.0509	0.0025	0.2894	0.0152	0.0411	0.0007	235.3	112.0	258.1	11.9	259.7	4.3	66
	WD17-003-4	18.74	342.4	347.8	0.9843	0.0517	0.0024	0.2809	0.0128	0.0398	0.0007	333.4	104.6	251.4	10.1	251.8	4.1	66

	元素	元素含量(×10 ⁻⁶)	(9-6				同位素比值	そ 比值					同位素年龄(Ma)	於(Ma)			
测点号	Ē	Ē	Ė	Th/U	$n(^{207}\text{Pb})/n(^{206}\text{Pb})$	n(206 Pb)	n(²⁰⁷ Pb),	$^{207}\text{Pb})/n(^{235}\text{U})$	$n(^{206}{ m Pb})/n(^{238}{ m U})$	$/n(^{238}\mathrm{U})$	$n(^{207}\text{Pb})/n(^{206}\text{Pb})$	ι(²⁰⁶ Pb)	$n(^{207}\text{Pb})/n(^{235}\text{U})$	ı(²³⁵ U)	$n(^{206}\text{Pb})/n(^{238}\text{U})$	(238U)	谐和度
	2	Пh	- -		测值	10	测值	1σ	测值	Ισ	测值	1σ	测值	1σ	测值	1σ	(%)
WD17-003-5	7.318	70.35	145.7	0.4829	0.0540	0.0037	0.2970	0.0187	0.0410	0.0008	368.6	155.5	264.0	14.6	258.9	5.2	86
WD17-003-6	10.62	80.07	205.0	0.3906	0.0524	0.0039	0.3117	0.0231	0.0430	0.0009	305.6	168.5	275.5	17.9	271.2	5.7	86
WD17-003-8	13.33	142.1	262.1	0.5424	0.0518	0.0028	0.2983	0.0153	0.0418	0.0008	276.0	122.2	265.1	12.0	263.9	4.7	66
WD17-003-9	11.80	234.1	210.8	1.111	0.0554	0.0040	0.2945	0.0191	0.0389	0.0008	427.8	161.1	262.1	15.0	245.8	4.9	93
WD17-003-10	12.23	134.8	243.7	0.553	0.0520	0.0029	0.2907	0.0153	0.0407	0.0008	287.1	125.9	259.1	12.0	257.4	4.7	66
WD17-003-11	8.999	194.0	181.8	1.067	0.0528	0.0051	0.2550	0.0249	0.0348	0.0008	320.4	218.5	230.7	20.2	220.6	4.9	95
WD17-003-12	8.331	71.24	166.8	0.427	0.0526	0.0035	0.2927	0.0197	0.0400	0.0008	322.3	151.8	260.7	15.5	253.0	5.1	26
WD17-003-13	8.544	105.3	173.8	909.0	0.0516	0.0052	0.2805	0.0279	0.0396	0.0012	333.4	231.5	251.0	22.1	250.2	7.6	66
WD17-003-15	5.452	85.98	101.7	0.8156	0.0566	0.0058	0.2984	0.0261	0.0397	0.0009	472.3	229.6	265.1	20.4	251.0	5.5	94
WD17-003-16	11.87	86.71	249.0	0.3482	0.0528	0.0030	0.2919	0.0170	0.0401	0.0007	320.4	136.1	260.0	13.3	253.3	4.4	26
WD17-003-17	9.975	100.2	207.9	0.4822	0.0554	0.0038	0.2999	0.0194	0.0398	0.0008	427.8	121.3	266.3	15.1	251.4	5.0	94
WD17-003-18	17.84	255.4	360.6	0.7085	0.0552	0.0038	0.2850	0.0184	0.0375	0.0007	420.4	155.5	254.6	14.5	237.5	4.3	93
WD17-003-19	16.52	179.9	341.2	0.5272	0.0538	0.0030	0.2964	0.0176	0.0396	0.0007	364.9	127.8	263.6	13.8	250.2	4.5	94
WD17-003-20	19.90	265.4	399.7	0.6641	0.0507	0.0037	0.2696	0.0193	0.0386	0.0008	233.4	165.7	242.4	15.5	244.1	5.2	66
WD17-003-21	18.83	272.4	354.4	0.7687	0.0526	0.0027	0.2858	0.0137	0.0396	9000.0	322.3	121.3	255.3	10.8	250.3	3.9	86
WD17-003-22	11.01	78.15	238.8	0.3272	0.0524	0.0048	0.2792	0.0261	0.0388	9000.0	301.9	211.1	250.0	20.7	245.2	3.9	86
WD17-003-24	10.58	97.64	213.4	0.4575	0.0527	0.0044	0.2874	0.0226	0.0401	0.0010	322.3	186.1	256.5	17.9	253.7	6.5	86
WD17-003-25	14.95	157.8	296.8	0.5317	0.0506	0.0026	0.2861	0.0152	0.0405	0.0006	220.4	123.1	255.5	12.0	256.2	3.5	66
WD17-003-26	14.34	173.1	275.4	0.6286	0.0528	0.0027	0.2975	0.0156	0.0407	0.0007	320.4	110.2	264.4	12.2	256.9	4.2	97

岩的 SiO, 含量介于 65%~70.06%, 在 TAS 图解中落入石英二长花岗岩和花岗 岩区域内,且显示为亚碱性、钙碱系列岩 浆(图 5a、c); Na, O 含量(5.16%~ 5.53%) 大于 K, O (2.57% ~ 3.16%), Na,O/K,O为 1.63~2.14, 富钠贫钾, 属 于钠质系列(图 5d); MgO 含量较高 (1.20%~1.91%), Mg[#]为52~59, 平均 为 56。 Al, O, 含量较高(15.17%~ 16.29%),铝饱和指数 A/CNK = 1.023~ 1.099.属于弱过铝质花岗岩(图 5b)。 微量元素具有高 Sr 低 Y 的特征, Sr 含量 为741.00×10⁻⁶~1198.83×10⁻⁶,平均为 979.85×10⁻⁶.Y含量为4×10⁻⁶~6.02× 10⁻⁶, Sr/Y 为 171.55~212.75, 平均为 176.78。稀土总量较低, LREE/HREE 变化范围为 10.50~13.30,轻重稀土分 馏明显,轻稀土富集,重稀土亏损;δEu 介于 1.14~1.46,显示弱的正銪异常(图 6a)

色尔崩岩体 SiO,含量介于 65.96% ~66.42%,相比努和亭沙拉岩体略低, 亚碱性系列, SiO,—TFeO/MgO 图解中 属钙碱系列岩浆(图 5a、c): 富钠 (5.30% ~ 5.35%) 贫钾(2.84% ~ 2.89%),Na₂O/K₂O 为 1.83~1.88,也是 钠质系列岩石(图 5d): MgO 含量为 1.49%~1.54%, Mg* 为 56~57, 平均为 56.5; 铝饱和指数 A/CNK = 0.969~ 1.008,在 A/CNK—A/NK 图解中落入准 铝质区域(图 5b)。微量元素具有高 Sr 和高 Sr/Y 的特点, Sr 含量为 817.39× 10⁻⁶ ~ 822. 29 × 10⁻⁶, 平均为 819. 79 × 10⁻⁶, Sr/Y 范围为119.99~137.77, 平均 为 128.38。LREE/HREE 变化范围为 13.63~14.73,轻重稀土分馏明显,轻稀 土富集,重稀土亏损;δEu 介于 1.06~ 1.41,显示弱的正銪异常(图 6a)。

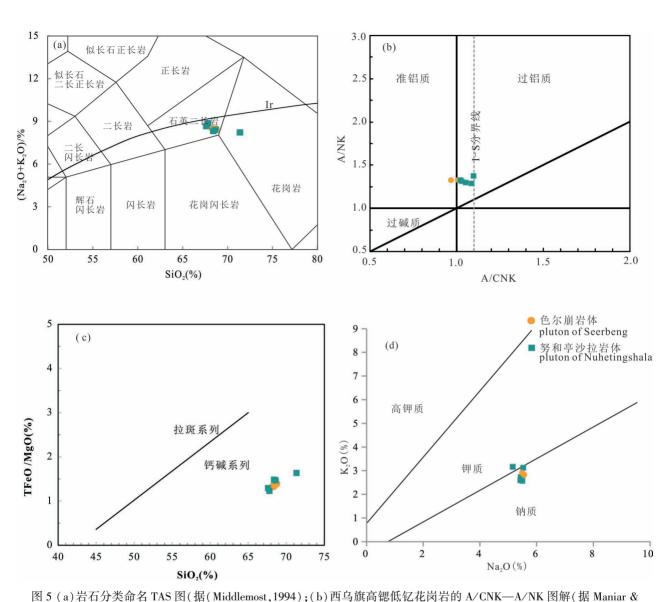
高锶低钇型中酸性岩(adakite,亦有人音译为埃达克岩)是一类具有特殊岩石化学特征的岩石类型,是 Defant 和Drummond(1990)在研究阿留申 Adak岛的富镁安山岩时提出来的,他们认为这种富镁安山岩可能是太平洋俯冲板片

表 2 西乌珠穆沁旗高锶低钇型花岗岩岩石化学分析结果 Table 2 Chemical compositions of granitoids in the West Ujimqin area

							3 J								
	<u></u>	色尔崩			努和亭沙拉				色尔崩	7崩			努和亭沙拉		
	SEB17-01	SEB17-02	WD17-003	WD17-003 WD17-004	WD17-005	X4066#	X0073#		SEB17-01	SEB17-02	WD17-003	WD17-004	WD17-005	X4066#	X0073#
				枯宮斑光								枯因斑形	_		
SiO_2		66.42	29.99	65	66.16	90.99	70.06	Ċ	37.89	20.00	13.92	64.97	30.40	51	29.7
${ m TiO}_2$		0.408	0.418	0.456	0.439	0.45	0.21	ï	13.39	13.51	7.59	30.91	26.46	17.7	14.7
$\mathrm{Al}_2\mathrm{O}_3$		15.71	16.29	15.73	16.12	15.36	15.17	La	17.03	16.44	11.84	13.67	13.34	10.00	8.00
${ m TFe}_2{ m O}_3$		2.31	2.39	2.7	2.61	2.97	2.18	g	30.33	33.39	25.29	26.02	29.79	23.00	18.00
M_{nO}	0.036	0.032	0.034	0.033	0.034	90.0	0.03	Pr	4.81	4.11	2.92	3.76	3.40	3.11	2.45
$M_{\rm gO}$		1.49	1.47	1.88	1.91	1.8	1.2	PΝ	14.12	15.78	10.73	11.44	12.56	11.00	00.6
CaO		2.04	1.61	1.91	1.55	1.74	1.17	Sm	2.54	2.63	1.99	2.08	2.26	2.13	1.67
Na_2O		5.35	5.43	5.16	5.53	5.43	5.5	Eu	1.01	98.0	0.70	0.87	0.82	0.72	0.59
K_2O		2.84	2.74	3.16	3.12	2.6	2.57	PS	1.87	2.32	1.75	1.59	2.09	1.61	1.35
P_2O_5		0.122	0.11	0.115	0.11	0.12	0.1	TP	0.25	0.26	0.22	0.22	0.24	0.24	0.17
烧失		2.98	1.99	2.98	1.55	3.11	1.53	Dy	1.13	1.20	1.10	1.07	1.19	1.13	0.94
向量		7.66	99.17	99.12	99.15	7.66	99.72	Но	0.20	0.22	0.21	0.20	0.22	0.23	0.17
$\rm Na_2O/K_2O$		1.88	1.98	1.63	1.77	2.09	2.14	Er	0.57	0.65	09.0	0.56	0.65	99.0	0.49
${ m Mg}^{*}$		99	55	28	59	55	52	Tm	0.09	0.09	0.08	0.09	0.09	0.10	0.07
Rb		46.16	43.54	53.74	47.16	38	36	Yb	0.54	0.56	0.54	0.54	0.58	0.70	0.50
Ba		953.94	665.23	983.56	1087.90	693.00	867.00	Lu	0.09	0.09	0.09	0.09	0.09	0.09	0.07
Th		6.20	6.11	0.02	7.28	6.10	5.60	Y	5.98	6.85	6.02	5.53	6.58	00.9	4.00
Ω		1.26	1.19	6.35	1.71			Sr/Y	136.77	119.99	199.30	173.26	171.55	123.50	212.75
Nb		2.19	2.02	2.36	2.42	2.50	2.50	ZREE	74.59	78.58	58.04	62.19	67.32	54.72	43.47
\mathbf{S}		822.19	1198.83	958.19	1128.57	741.00	851.00	LREE/HREE	14.73	13.63	11.70	13.30	12.08	10.50	10.56
$_{ m N}$	14.12	15.78	10.73	11.44	12.56	11.00	00.6	$\mathrm{La}_\mathrm{N}/\mathrm{Yb}_\mathrm{N}$	22.51	21.15	15.84	18.15	16.47	10.25	11.48
Zr	125.47	144.38	125.65	120.84	139.07	114	107	δEu	1.41	1.06	1.14	1.46	1.16	1.19	1.20
JH	3.58	3.80	3.27	3.37	3.64	3.30	3.20								
	,,						(0 17)								

注: $Mg^* = \frac{n(\text{Mg})}{n(\text{Mg}) + n(\text{TFe})}$; A/CNK = $\frac{n(\text{Mg})}{n(\text{CaO}) + n(\text{Na}_2\text{O}) + n(\text{Na}_2\text{O})}$; A/NK = $\frac{n(\text{Na}_2\text{O})}{n(\text{Na}_2\text{O}) + n(\text{K}_2\text{O})}$; X4066*和 X0073*源自沈阳地 $n({\rm Al}_20_3)$ $n({\rm Al}_2{\rm O}_3)$ $n(\mathrm{Mg})$

质矿产研究所 ,表中空白处为未测数据。



Piccoli, 1989);(c) 岩浆 FeOT/MgO—SiO₂ 图解(Miyashiro,1974);(d) Na₂O—K₂O 图解(据 Middlemost, 1975)
Fig. 5 (a) Total alkali—silica (TAS) diagram of the late Permian rocks;(b) A/CNK versus A/NK diagram (after Maniar & Piccoli,1989) of granitoids; (c) FeOT/MgO—SiO₂ diagram of granitoids (after Miyashiro 1974);(d) Na₂O—K₂O diagram (after Maniar & Piccoli,1989) of granitoids; (c) FeOT/MgO—SiO₂ diagram of granitoids (after Miyashiro 1974);(d) Na₂O—K₂O diagram (after Miyashiro 1974);

熔融形成的,是俯冲消减环境中的一类特殊岩石。本次研究发现色尔崩和努和亭沙拉晚二叠世岩浆岩具有相似的地球化学性质,且符合岛弧 adakite 的特征,主要表现为: $SiO_2>57\%$ (65.00%~70.06%), $Al_2O_3>15\%$ (15.54%~16.29%),MgO<3%(1.20%~1.91%), $Mg^{\#}$ 为52~59。微量元素高Sr($Sr>741×10^{-6}$)和Sr/Y,低Y和Yb,Sr/Y范围为93.1~212.75,微量元素原始地幔蛛网图中有明显Sr的峰值和Nb、Ta的亏损。稀土元素富集LREE亏损HREE,轻重稀土分异显著,Eu 弱的正异常,这些地

Middlemost, 1975)

球化学特征指示岩体具有 adakite 的性质(Defant and Drummond 1990)。同时,在 Yb_N —(La/Yb) $_N$ 判别图解和 Sr/Y—Y 判别图中,样品均落入 adakite 岩范围内(图 7)。综上所述,西乌旗晚二叠世花岗斑岩岩应为高锶低钇型中酸性岩。

4.3 锆石 Hf 同位素分析结果

在锆石 U-Pb 测年基础上进行了 Lu-Hf 同位素分析,分析结果显示(表 3),两个样品所有锆石的 n (176 Hf)/n(177 Hf)比值均小于 0.002,表明锆石形成后具有极低量的放射成因 Hf。其中,样品(SEB17-

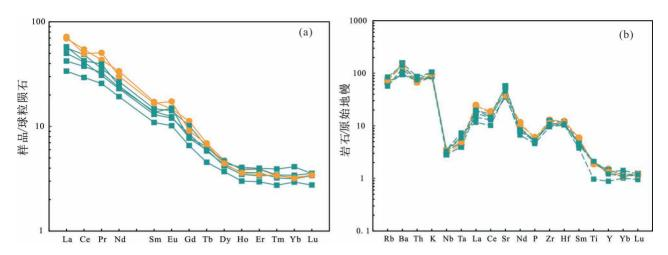


图 6 (a) 稀土元素球粒陨石标准化分布图和(b) 微量元素原始地幔标准化蛛网图 (原始地幔标准化值和球粒陨石标准化值据 Sun and Mcdonough, 1989;图例同图 5a)

Fig. 6 (a) Chondrite-normalized REE pattern diagrams and (b) Primitive mantle normalized incompatible element pattern diagrams of granitoids in West Ujimqin area(after Sun and Mcdonough, 1989)

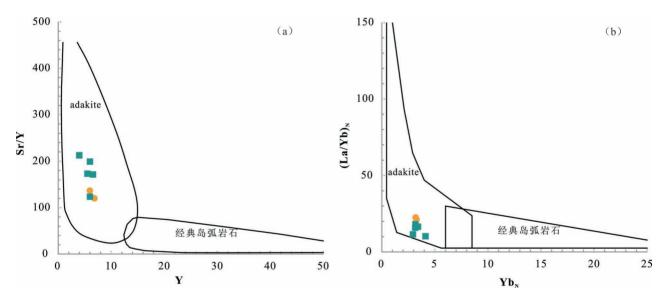


图 7 (a) 西乌旗二叠世花岗岩 Sr/Y—Y 图解(据 Martin,1999)和(b) (La/Yb)_N—Yb_N (据 Defant and Drummond,1990; 图例同图 6a)

Fig. 7 Diagrams of Sr/Y—Y (a) and (La/Yb) $_{\rm N}$ —(Yb) $_{\rm N}$ (b) for granitoids in West Ujimqin area (after Defant and Drummond, 1990)

02) $n(^{176}$ Hf $)/n(^{177}$ Hf) 的变化范围为 $0.282922 \sim 0.282994$,平均为 0.282942。对应的 $\varepsilon_{\rm Hf}(t)$ 值在 $+9.8 \sim +13.3$,亏损地幔模式年龄 $(T_{\rm DM1})$ 为 $363 \sim 510$ Ma,二阶段模式年龄 $T_{\rm DM2}$ 为 $429 \sim 655$ Ma。样品 (WD17-03) 中 $n(^{176}$ Hf $)/n(^{177}$ Hf) 的变化范围为 $0.282849 \sim 0.283002$,平均为 0.282939,亏损地幔模式年龄 $(T_{\rm DM1})$ 为 $353 \sim 577$ Ma,二阶段模式年龄 $(T_{\rm DM2})$ 为 $430 \sim 764$ Ma,平均为 559 Ma。

5 讨论

5.1 岩浆岩的形成时代

努和亭沙拉岩体侵入中二叠统哲斯组和下二叠统寿山沟组中,在岩体西部,下白垩统梅勒图组不整合于其上,1:25万区域地质调查报告将其划为侏罗纪侵入岩体[●]。本次研究选取努和亭沙拉东南部花岗斑岩(WD17-003)进行锆石 U-Pb 定年,获得的

表 3 锆石原位 Lu-Hf 同位素分析结果

Table 3 Zircon Lu-Hf isotopic compositions of granite in West Ujimqin area

							,					
点号	年龄 (Ma)	$\frac{n({}^{176}\text{Yb})}{n({}^{177}\text{Hf})}$	2σ	$\frac{n(^{176}\text{Lu})}{n(^{177}\text{Hf})}$	2σ	$\frac{n({}^{176}\text{Hf})}{n({}^{177}\text{Hf})}$	2σ	$arepsilon_{ ext{Hf}}(0)$	$arepsilon_{ ext{Hf}}(t)$	T _{DM1} (Ma)	T _{DM2} (Ma)	$f_{ m Lu/Hf}$
SEB17-02-01	258	0.010167	0.000150	0.000395	0.000004	0.282937	0.000015	5.84	11.4	439	552	-0.99
SEB17-02-02	256	0.028403	0.000276	0.001122	0.000010	0.282954	0.000019	6.44	11.9	423	522	-0.97
SEB17-02-03	256	0.020929	0.000143	0.000802	0.000002	0.282946	0.000019	6.15	11.7	431	538	-0.98
SEB17-02-04	257	0.021254	0.000352	0.000819	0.000011	0.282951	0.000018	6.33	11.8	424	526	-0.98
SEB17-02-05	257	0.020368	0.000214	0.000788	0.000005	0.282928	0.000016	5.53	11.0	456	577	-0.98
SEB17-02-06	257	0.016446	0.000262	0.000645	0.000009	0.282940	0.000018	5.95	11.5	438	548	-0.98
SEB17-02-07	257	0.024220	0.000242	0.000946	0.000007	0.282922	0.000016	5.31	10.8	467	593	-0.97
SEB17-02-08	254	0.013408	0.000099	0.000521	0.000002	0.282941	0.000018	5.97	11.5	436	548	-0.98
SEB17-02-09	245	0.017827	0.000282	0.000706	0.000008	0.282954	0.000018	6.42	11.7	419	526	-0.98
SEB17-02-11	255	0.020692	0.000335	0.000838	0.000009	0.282994	0.000017	7.86	13.3	363	429	-0.97
SEB17-02-12	255	0.025314	0.000218	0.001014	0.000008	0.282935	0.000017	5.78	11.2	449	565	-0.97
SEB17-02-13	258	0.046842	0.000571	0.001563	0.000012	0.282897	0.000019	4.44	9.8	510	655	-0.95
SEB17-02-14	254	0.025436	0.000208	0.001053	0.000012	0.282952	0.000019	6.37	11.8	425	528	-0.97
SEB17-02-15	259	0.017776	0.000139	0.000696	0.000006	0.282938	0.000016	5.87	11.5	441	553	-0.98
WD17-003-01	256	0.036117	0.000857	0.001340	0.000030	0.282849	0.000019	2.72	8.1	577	764	-0.96
WD17-003-02	254	0.018809	0.000492	0.000745	0.000014	0.282994	0.000019	7.84	13.3	363	430	-0.98
WD17-003-03	245	0.024023	0.000330	0.000965	0.000016	0.282941	0.000025	5.98	11.2	440	557	-0.97
WD17-003-04	250	0.054810	0.001052	0.002196	0.000036	0.282858	0.000027	3.04	8.2	577	756	-0.93
WD17-003-05	250	0.035566	0.000291	0.001480	0.000010	0.282961	0.000024	6.67	11.9	418	515	-0.96
WD17-003-06	238	0.022620	0.000485	0.000958	0.000022	0.283002	0.000026	8.14	13.2	353	423	-0.97
WD17-003-07	251	0.014627	0.000384	0.000566	0.000012	0.282951	0.000019	6.33	11.8	422	527	-0.98
WD17-003-08	253	0.022933	0.000222	0.000837	0.000011	0.282987	0.000020	7.60	13.0	374	447	-0.97
WD17-003-09	251	0.017935	0.000167	0.000739	0.000013	0.282904	0.000020	4.68	10.1	489	634	-0.98
WD17-003-10	257	0.020060	0.000481	0.000819	0.000021	0.282937	0.000021	5.82	11.3	445	559	-0.98
WD17-003-11	250	0.019692	0.000266	0.000808	0.000006	0.282984	0.000023	7.48	12.9	378	456	-0.98
WD17-003-12	257	0.016885	0.000103	0.000696	0.000004	0.282952	0.000018	6.36	11.9	422	523	-0.98
WD17-003-13	246	0.037036	0.000335	0.001552	0.000019	0.282903	0.000021	4.64	9.8	502	649	-0.95
WD17-003-14	271	0.024930	0.000107	0.000969	0.000004	0.282959	0.000019	6.60	12.4	415	502	-0.97
WD17-003-15	259	0.022860	0.000585	0.000990	0.000029	0.282902	0.000021	4.60	10.1	496	638	-0.97

注:表中参数计算公式及常数取值如下:

$$\begin{split} \varepsilon_{\mathrm{Hf}}(t) &= 10000 \cdot \left\{ \frac{\left[\frac{n^{(176\,\mathrm{Hf})}}{n^{(177\,\mathrm{Hf})}} \right]_{\mathrm{S}}^{-} \left[\frac{n^{(176\,\mathrm{Lu})}}{n^{(177\,\mathrm{Hf})}} \right]_{\mathrm{S}}^{-} \cdot \left(\mathrm{e}^{\lambda t} - 1 \right)}{\left[\frac{n^{(176\,\mathrm{Lu})}}{n^{(177\,\mathrm{Hf})}} \right]_{\mathrm{CHUR},0}^{-} - \left[\frac{n^{(176\,\mathrm{Lu})}}{n^{(177\,\mathrm{Hf})}} \right]_{\mathrm{CHUR}}^{-} \cdot \left(\mathrm{e}^{\lambda t} - 1 \right)}{\left[\frac{n^{(176\,\mathrm{Lu})}}{n^{(177\,\mathrm{Hf})}} \right]_{\mathrm{CHUR}}^{-} - \left[\frac{n^{(176\,\mathrm{Lu})}}{n^{(177\,\mathrm{Hf})}} \right]_{\mathrm{CHUR}}^{-} - 1} \right\}_{\mathrm{CHUR}}^{-} \\ T_{\mathrm{DM}\,2\mathrm{CC}} &= T_{\mathrm{DMI}} - \left(T_{\mathrm{DMI}} - t \right) \cdot \frac{f_{\mathrm{CC}} - f_{\mathrm{S}}}}{f_{\mathrm{CC}} - f_{\mathrm{DM}}}; f_{\mathrm{La}/\mathrm{Hf}} = \frac{\left[\frac{n^{(176\,\mathrm{Lu})}}{n^{(177\,\mathrm{Hf})}} \right]_{\mathrm{S}}^{-} - 1}{\left[\frac{n^{(176\,\mathrm{Lu})}}{n^{(177\,\mathrm{Hf})}} \right]_{\mathrm{CHUR}}^{-} - 1} \\ &= \frac{\left[\frac{n^{(176\,\mathrm{Lu})}}{n^{(177\,\mathrm{Hf})}} \right]_{\mathrm{CHUR}}^{-} - 1}{\left[\frac{n^{(176\,\mathrm{Lu})}}{n^{(177\,\mathrm{Hf})}} \right]_{\mathrm{S}}^{-} + 1} \\ &= \frac{1}{n^{(176\,\mathrm{Lu})}} \left[\frac{1}{n^{(176\,\mathrm{Hf})}} \right]_{\mathrm{CHUR}}^{-} - 1 \\ &= \frac{1}{n^{(176\,\mathrm{Lu})}} \right]_{\mathrm{CHUR}}^{-} - 1 \\ &= \frac{1}{n^{(176\,\mathrm{Lu})}} \left[\frac{1}{n^{(176\,\mathrm{Hf})}} \right]_{\mathrm{CHUR}}^{-} - 1 \\ &= \frac{1}{n^{(176\,\mathrm{Lu})}} \left[\frac{1}{n^{(176\,\mathrm{Hf})}} \right]_{\mathrm{CHUR}}^{-} - 1 \\ &= \frac{1}{n^{(176\,\mathrm{Lu})}} \right]_{\mathrm{CHUR}}^{-} - 1 \\ &= \frac{1}{n^{(176\,\mathrm{Lu})}} \left[\frac{1}{n^{(176\,\mathrm{Hf})}} \right]_{\mathrm{CHUR}}^{-} - 1 \\ &= \frac{1}{n^{(176\,\mathrm{Lu})}} \right]_{\mathrm{CHUR}}^{-} - 1 \\ &= \frac{1}{n^{(176\,\mathrm{Lu})}} \left[\frac{1}{n^{(176\,\mathrm{Hf})}} \right]_{\mathrm{CHUR}}^{-} - 1 \\ &= \frac{1}{n^{(176\,\mathrm{Lu})}} \right]_{\mathrm{CHUR}}^{-} - 1 \\ &= \frac{1}{n^{(176\,\mathrm{Lu})}} \left[\frac{1}{n^{(176\,\mathrm{Hf})}} \right]_{\mathrm{CHUR}}^{-} - 1 \\ &= \frac{1}{n^{(176\,\mathrm{Lu})}} \right$$

²⁰⁶Pb/²⁰⁸U加权平均年龄为 254. 4±1. 2 Ma,属于晚二 叠世。

色尔崩花岗斑岩(SEB17-02)锆石 LA-ICP-MS U-Pb 年龄为 255.3±0.7 Ma,与努和亭沙拉年龄接近。色尔崩小岩株呈不规则状侵入于中二叠世大石寨组和哲斯组,侵入体边部见哲斯组灰色生物碎屑灰岩,其形成年龄应该晚于中二叠世,与锆石定年相符。两个岩体区域上地理位置相近,岩石学和岩石地球化学相似,成岩年龄相近,应为晚二叠世同一岩浆构造活动的产物。

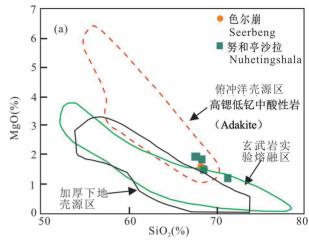
区域上,张玉清(2009)在苏左旗巴音乌拉识别出了岛弧型"埃达克质"花岗闪长岩,获得的锆石LA-ICP-MS U-Pb 年龄为 256. 1±0.9 Ma。李承东等(2007)在吉林色洛河地区岛弧型高镁安山岩中获得了 252±5 Ma 的 SHRIMP 锆石 U-Pb 年龄,为晚二叠世。Gao Xiaofeng 等(2016)首次在西乌旗地区识别出了 251~253 Ma 的安山岩,且这些安山岩具有高锶低钇型中酸性岩的特征,与本文研究的侵入岩一起组成了晚二叠世高锶低钇型中酸性火成岩。因此,西乌旗地区确实存在一期晚二叠世的构造岩浆活动。

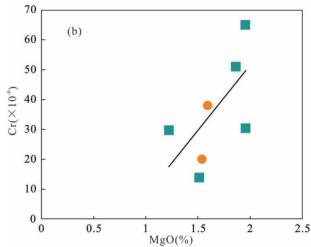
5.2 岩石成因类型及源区性质

由原始定义可以看出, adakite 是一种具有特殊岩石地球化学特征和构造环境的岩石系列(Defant and Drummond, 1990)。随着研究的深入, 越来越多的学者认为 adakite 不仅可以产生在原始定义的岛弧环境,新生下地壳的部分熔融和玄武岩底侵作用、下地壳的拆沉作用同样可以形成 adakite (Peacock et al., 1994; Petford and Atherton, 1996; 许继峰等, 2014), 并通过蚀变玄武岩的部分熔融实验进行了验证(Atherton and Petford, 1993; Rapp et al., 2002)。因此, 高锶低钇型中酸性岩浆既可以来源于俯冲板片的熔融, 也可以形成于新生下地壳的熔融。

Mg[#]值被认为是判断高锶低钇型中酸性岩岩浆源区的一个重要参数(Rapp et al.,1999)。由下地壳铁镁质岩石直接部分熔融所形成的岩浆,其 Mg[#]值一般不会超过 40, MORB 部分熔融产生的熔体的Mg[#]值也不会超过 45,而由 MORB 产生的熔体如在上升过程中与地慢楔发生交代作用,其 Mg[#]值可超过 50(肖庆辉等,2002;许立权等,2003,Atherton and Petord. 1993)。许继峰(2014)认为来源于下地壳直接熔融形成的 adakite 共同特征是具有低的 Mg[#]。西乌旗高锶低钇型花岗岩具有较高的 MgO 含量和

Mg[#], Mg[#]为52~59, 平均为56, 高于 MORB 部分熔融 形成的 adakite, 也高于下地壳熔融来源的 adakite,





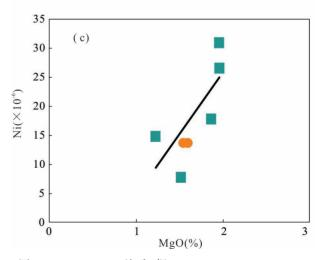


图 8 (a) SiO₂—MgO 关系(据 Yu Shengyao et al.,2015); (b) MgO—Cr 协变关系图解;(c) MgO—Ni 协变关系图解 Fig. 8 (a) SiO₂ versus MgO diagram (modified from Yu Shengyao et al.,2015); (b) MgO versus Cr diagram;(c) MgO versus Cr diagram

如华北克拉通底侵作用形成的"埃达克质岩" Mg[#]约为 35.72~46.16(张旗等,2001; 罗红玲等,2007; 熊小林等,2011)。西乌旗晚二叠世高锶低钇花岗岩与兴蒙造山带内早古生代俯冲板片熔融的"埃达克质岩"具有相似特征,MgO 含量和 Mg[#]均较高(表4,图 8a)。这种现象一般认为是俯冲板片熔融形成的高锶低钇型中酸性岩浆熔体上升过程中与上覆地幔楔发生交代反应,增加了 Mg 的含量(Sen and Dunn.,1994; Rapp et al.,1999)。在 SiO₂—MgO 关系图解中,本文高锶低钇花岗岩都落在俯冲洋壳范围内(图 8a),应属于俯冲洋壳(MORB)部分熔融形成的高锶低钇花岗斑岩。

高锶低钇型中酸性岩中代表幔源成分的 Cr、Ni等相容元素与 MgO 的含量呈正相关性(图 8b、c),表明高锶低钇型中酸性岩融体在上升过程中与地幔橄榄岩发生了交代作用。微量元素原始地幔蛛网图中,大离子亲石元素(LILE)相对富集,Nb、Ta、Ti、P等高场强元素相对亏损,显示具有俯冲带岩浆岩的特征。因此,本文高锶低钇型中花岗斑岩不是来源于下地壳重融而是含水的俯冲板片熔融交代的结果。

锆石 Hf 同位素在示踪岩浆源区方面具有重要作用(吴福元等,1999)。高锶低钇型花岗岩中 $\varepsilon_{Hf}(t)$ 值全部为正值(+8.1~+13.3),显示岩浆来源于亏损地幔或新生下地壳,Hf 同位素特征与兴蒙造山带东段幔源岩浆岩 Hf 的演化一致(图 9)(Yang Jinhui et al., 2006; 刘建峰等,2014),显示与兴蒙造山带东段显生宙岩浆岩类似的同位素组成特征。两个岩体的锆石单阶段模式年龄介于353~577 Ma.

与区域内早古生代蛇绿岩的年龄范围一致(包志伟等,1994;刘敦一等,2003),表明早古生代古亚洲洋洋壳可能为高锶低钇花岗岩的源区。

5.3 构造环境及地质意义

研究区内,古亚洲洋经历了复杂的演化过程。李英杰等(2017)在西乌旗迪彦庙蛇绿岩中识别出前孤玄武岩、岛弧拉斑玄武岩和玻安岩,指示形成于前弧环境,而前弧玄武岩的锆石年龄为333.4 Ma,代表古亚洲洋在石炭纪发生了洋内俯冲作用。随着古亚洲洋的俯冲,在迪彦庙—达青牧场蛇绿岩带北部形成了苏左旗—西乌旗石炭纪岛弧岩浆岩带(陈斌等,2001;刘建峰等,2009; Wang Limin et al.,2014);同时,康健丽等(2016)在锡林浩特地区发现岛弧型变质基性火山岩,其锆石 U-Pb 年龄为323~334 Ma,区域岩石组合表明古亚洲洋石炭纪存在向北俯冲消减。

在早、中二叠世北部地区(蒙古地块的南缘)产生了拉张,不同地区表现形式不一样。白音乌拉一东乌旗形成了 A 型花岗岩带,在西乌旗地区则有双峰式火山岩的发育(洪大卫等,1994; Zhang Xiaohui et al.,2008)。赵英利等(2016)研究了内蒙东部地区中二叠统哲斯组沉积岩,发现碎屑成分差别不大,且来自华北克拉通的锆石很少,认为古亚洲洋在中二叠世时仍然存在一个开放的大洋。

从区域地层看,晚二叠世开始,西乌旗地区在强烈挤压应力作用下整体抬升,缺失该时期的沉积地层,并在石炭系—二叠系地层中形成了 NE 向褶皱、断裂、韧性剪切带等构造[●],南部晚二叠世林西组地层也开始出现从海相到陆相过渡的特征(和政军

表 4 内蒙古洋壳俯冲型 adakite 特征值对比
Table 4 Comparison of adakite rock from Inner Mongolia

类别		į	兴蒙造山带 adakite	e		典型。	adakite
地点	达茂旗	正镶白旗	梅劳特乌拉	巴音乌拉	西乌旗	I 类 adakite	II类 adakite
时代	450 Ma	457±11 Ma	294.7±1.7 Ma	256.1± 0.9 Ma	256 Ma		
岩性	闪长岩	二长花岗岩	花岗闪长岩	花岗闪长岩	花岗斑岩		
${\rm SiO_2}$	56.76~69.24	73.52~74.68	64.93~69.50	62.13~72.87	65~66.67	≥56.00	56.06~72.48
MgO	1.08~3.07	0.29~0.39	0.8~1.48	0.48~2.95	1.47~1.91	<3	0.1~2.56
Sr	657 ~ 1232	435.4~719.7	368~700	425.1~645.2	741~1128	>400	355~1512
Sr/Y	43~876	104~177	49~111	45~59	120~212	>20~40	38~617
$(La/Yb)_N$	5.3~38.7	8.3~16.9	3.3~5.1	8.5~15.1	10.3~21.2	≥10	26~142.9
$Mg^{\#}$	38~48	31.22~57.78	42~52	46.61~82.45	56~59	>47	小于 50
样品数	n = 7	n = 4	n = 5	n = 8	n = 5		
资料来源	许立权等, 2003	秦亚等, 2013	王金芳等, 2017	张玉清等,2009	本次实验		

注:典型 adakite 地球化学特征转引自裴先治(2003), I 类 adakite 为俯冲板片熔融形成的 adakite, II 类 adakite 为底侵形成的 adakite。

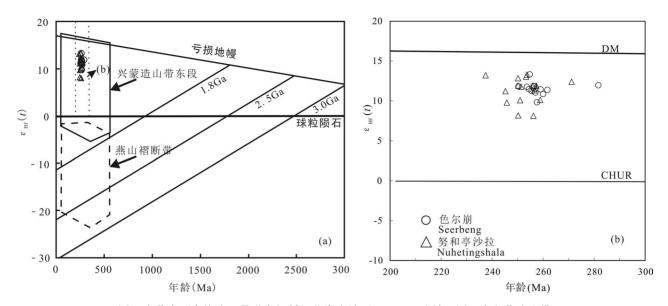


图 9 内蒙古西乌旗晚二叠世高锶低钇花岗岩锆石 $\varepsilon_{\rm Hf}(t)$ —t 图解(图 a 中兴蒙造山带东段和燕山褶断带岩浆岩锆石 $\varepsilon_{\rm Hf}(t)$ 范围据 Yang Jinhui et al., 2006)

Fig. 9 Zircon $\varepsilon_{\rm Hf}(t)$ —t diagrams of Late Permian adakite in West Ujimqin area (the fields of zircon $\varepsilon_{\rm Hf}(t)$ values of magmatic rocks from the eastern Yanshan Fold and Thrust Belt are after Yang Jinhui et al., 2006)

等,1997),说明古亚洲洋接近闭合,此时可能不存在大规模的洋壳板片俯冲。而研究区的高锶低钇型花岗斑岩位于火山弧的构造环境中(图9),可能是俯冲板片断离后,在俯冲带下方发生部分熔融,形成的岩浆熔体在上升过程中与地幔楔橄榄岩发生反应,侵入到上地壳形成高锶低钇型花岗岩。同时,研究区内还识别出同时代的具有高锶低钇型中酸性岩

特征的高镁安山岩(Gao Xiaofeng et al.,2016),与高 锶低钇花岗斑岩共同构成了俯冲板片断离构造背景下的火成岩组合。

区域上,研究区西部的索伦缝合带在晚二叠世(约250 Ma)也发生了俯冲板片断离,俯冲板片部分熔融产生的熔体与地幔橄榄岩充分反应,形成了高镁安山岩(Jian Ping et al.,2010)。同时,东部吉林

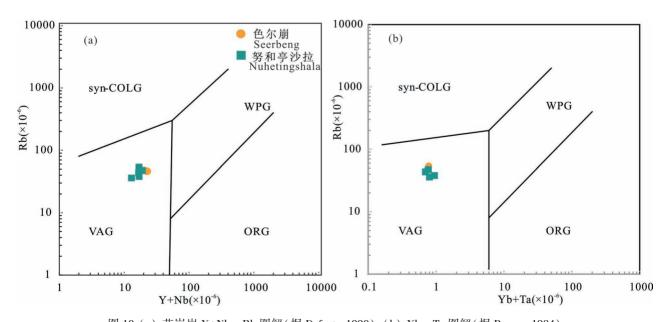


图 10 (a) 花岗岩 Y+Nb—Rb 图解(据 Defant, 1990);(b) Yb—Ta 图解(据 Pearce, 1984)

Fig. 10 Y+Nb—Rb diagram of granitiods (after Defant, 1990); (b) Yb—Ta diagram of granitiods (after Pearce, 1984)

色洛河也发育同期的高镁安山岩(李承东等, 2007)。内蒙古晚古生代的 adakite 和高镁安山岩及镁安山岩的岩石组合,表明晚二叠世存在洋壳的俯冲,且俯冲洋壳在碰撞前可能发生了断离。

古亚洲洋的闭合是一个漫长的过程,石炭纪岩浆弧和蛇绿岩,说明大洋在石炭纪就已经开始俯冲消减,晚二叠世弧岩浆岩的存在,说明洋在继续俯冲消减。而二叠纪早期的 A 型花岗岩带 (洪大卫等,1994)位于本文研究区的西北部,不能否定南部还有洋的俯冲存在。南部双井地区,中三叠世碰撞型花岗岩的出现(李锦轶等,2007),说明古亚洲洋在中三叠世已经闭合,其最终缝合位置可能为索伦—西拉木伦一线。

6 结论

- (1)努和亭沙拉花岗岩岩体的形成时间为254.4±3.4 Ma,色尔崩花岗岩形成时代为255.3±1.4 Ma,均为晚二叠世晚期。
- (2)努和亭沙拉花岗岩和色尔崩花岗斑岩具有富钠贫钾,高 Sr、低 Yb 与 Y 和高 Sr/Y 的特点,岩浆源区为俯冲洋壳部分熔融形成的高锶低钇型花岗岩 (adakitic granite)。Mg[#]较高,岩浆熔体可能与地幔橄榄岩发生了相互作用。
- (3)晚二叠世,高锶低钇花岗岩和高镁安山岩 形成于俯冲板片断离的构造背景下,古亚洲洋在晚 二叠世依然存在向北的俯冲消减,其最终闭合碰撞 可能发生在二叠纪之后。

致谢: 首先,感谢刘翠教授、石玉若研究员在成 文过程中提出的建议和帮助。然后,感谢审稿专家 及章雨旭研究员在论文修改中提供的宝贵意见。感 谢南京大学内生金属矿床成矿机制研究国家重点实 验室和中国地质大学(北京)的专家们在实验测试 中给与的帮助。

注释 / Note

● 沈阳地质矿产研究所. 2005. 西乌珠穆沁旗幅 1:25 万区域地质调查报告.

参考文献/References

- (The literature whose publishing year followed by a "&" is in Chinese with English abstract; The literature whose publishing year followed by a "#" is in Chinese without English abstract)
- 包志伟,陈森煌,张祯堂. 1994. 内蒙古贺根山地区蛇绿岩稀土元素和 Sm-Nd 同位素研究.地球化学,23(4):339~349.
- 陈斌,赵国春, Wilde S.2001. 内蒙古苏尼特左旗南两类花岗岩同位 素年代学及其构造意义. 地质论评, 47(4):361~367.

- 洪大卫,黄怀曾,肖宜君,徐海明,靳满元.1994.内蒙古中部二叠纪碱性花岗岩及其地球动力学意义.地质学报,68(3):219~230.
- 侯可军,李延河,邹天人,曲晓明,石玉若,谢桂青.2007.LA-MC-ICP-MS 锆石 Hf 同位素的分析方法及地质应用.岩石学报,23 (10):2595~2604.
- 和政军, 刘淑文,任纪舜,王瑜. 1997. 内蒙古林西地区晚二叠世—早 三叠世沉积演化及构造背景. 中国区域地质, 16(4): 403~409.
- 康健丽,肖志斌,王惠初,初航,任云伟,刘欢,高知睿,孙义伟.2016. 内蒙古锡林浩特早石炭世构造环境:来自变质基性火山岩的年 代学和地球化学证据.地质学报,90(2):383~397.
- 李承东,张福勤,苗来成,颉航强,许雅雯.2007.吉林色洛河晚二叠 世高镁安山岩 SHRIMP 锆石年代学及其地球化学特征.岩石学报,23(4):767~776.
- 李锦轶,高立明,孙桂华,李亚萍,王彦斌.2007.内蒙古东部双井子中三叠世同碰撞壳源花岗岩的确定及其对西伯利亚与中朝古板块碰撞时限的约束.岩石学报,23(3);565~582.
- 李锦轶,张进,杨天南,李亚萍,孙桂华,朱志新,王励嘉.2009.北 亚造山区南部及其毗邻地区地壳构造分区与构造演化.吉林大 学学报(地球科学版),39(4):584~605.
- 李双林,欧阳自远.1998.兴蒙造山带及邻区的构造格局与构造演化. 海洋地质与第四纪地质,18(3):46~55.
- 李英杰,王金芳,王根厚,李红阳,董培培.2018.内蒙古迪彦庙蛇绿岩带达哈特前弧玄武岩的发现及其地质意义.岩石学报,34(2):469~482.
- 刘敦一, 简平, 张旗, 张福勤, 石玉若, 施光海, 张履桥, 陶华.2003. 内蒙古图林凯蛇绿岩中埃达克岩 SHRIMP 测年: 早古生代洋壳消减的证据. 地质学报,77(3):317~327+435~437.
- 刘建峰, 迟效国, 张兴洲, 马志红, 赵芝, 王铁夫, 胡兆初, 赵秀羽. 2009.内蒙古西乌旗南部石炭纪石英闪长岩地球化学特征及其构造意义. 地质学报,83(3):365~376.
- 刘建峰,李锦轶,迟效国,曲军峰,胡兆初,郭春丽.2014.内蒙古东南部早三叠世花岗岩带岩石地球化学特征及其构造环境. 地质学报,88(9):1677~1690.
- 罗红玲, 吴泰然, 李毅.2007.乌拉特中旗克布岩体的地球化学特征 及 SHRIMP 定年:早二叠世华北克拉通底侵作用的证据. 岩石学报.23(4):755~766.
- 吕洪波, 冯雪东, 王俊, 朱晓青, 董晓朋, 张海春, 章雨旭. 2018. 狼山发现蛇绿混杂岩———华北克拉通与中亚造山带碰撞边界的关键证据. 地质论评,64(4):777~805.
- 裴先治,王涛,丁仨平,李勇,胡波.2003.东秦岭商丹带北侧新元古 代埃达克质花岗岩及其地质意义.中国地质,30(4);372~381.
- 秦亚,梁一鸿,邢济麟,张青伟,刘城先.2013.内蒙古正镶白旗地区 早古生代 O 型埃达克岩的厘定及其意义. 地学前缘,20(5):106 ~114.
- 石玉若, 刘翠, 邓晋福, 简平.2014.内蒙古中部花岗质岩类年代学格 架及该区构造岩浆演化探讨. 岩石学报.30(11):3155~3171.
- 孙德有,吴福元,张艳斌,高山.2004. 西拉木伦河—长春—延吉板块缝合带的最后闭合时间——来自吉林大玉山花岗岩体的证据. 吉林大学学报(地球科学版),34(2);174~181.
- 陶继雄,许立权,贺锋,苏茂荣.2005.内蒙古巴特敖包地区早古生代 洋壳消减的岩石证据. 地质调查与研究,28(1):1~8.
- 王冬兵,刘勇胜,宗克清,高长贵,徐娟.2009.内蒙古林西早中生代 0 型高镁埃达克质安山岩的发现及其意义. 地质科技情报,28(6):31~38.
- 王金芳,李英杰,李红阳,董培培.2017.内蒙古梅劳特乌拉蛇绿岩中 埃达克岩的发现及其演化模式.地质学报,91(8):1776~1795.
- 王强, 赵振华, 熊小林, 许继锋.2001.底侵玄武质下地壳的熔融:来 自安徽沙溪 adakite 质富钠石英闪长玢岩的证据. 地球化学.30

- $(4):353 \sim 362.$
- 王荃.1986.内蒙古中部中朝与西伯利亚古板块间缝合线的确定. 地质学报,(1):31~43.
- 王荃, 刘雪亚, 李锦轶.1991.中国内蒙古中部的古板块构造. 中国地质科学院院报,(1):1~15.
- 汪相. 2018. 白云鄂博超大型稀土—铌—铁矿床的成矿时代及成因 探析———兼论 P—T 之交生物群灭绝事件和"阿蒙兴造山运动". 地质论评,64(2):299~345.
- 王玉净, 樊志勇.1997. 内蒙古西拉木伦河北部蛇绿岩带中二叠纪放射虫的发现及其地质意义.古生物学报,36(1):58~69.
- 吴福元, 孙德有, 林强.1999.东北地区显生宙花岗岩的成因与地壳增生. 岩石学报,15(2): 181~189.
- 肖文交, 舒良树, 高俊, 熊小林, 王京彬, 郭召杰, 李锦轶, 孙敏. 2008.中亚造山带大陆动力学过程与成矿作用. 新疆地质, 26 (1):4~8.
- 熊小林, 刘星成, 朱志敏, 李元, 肖万生, 宋茂双, 张生, 吴金花. 2011.华北埃达克质岩与克拉通破坏:实验岩石学和地球化学依据, 中国科学·地球科学(5).654~667.
- 徐备,赵盼,鲍庆中,周永恒,王炎阳,罗志文.2014.兴蒙造山带前中生代构造单元划分初探. 岩石学报,30(7):1841~1857.
- 许继峰, 邬建斌, 王强, 陈建林, 曹康.2014.埃达克岩与埃达克质岩 在中国的研究进展. 矿物岩石地球化学通报, 33(1):6~13.
- 许立权, 邓晋福, 陈志勇, 陶继雄.2003.内蒙古达茂旗北部奥陶纪埃达克岩类的识别及其意义. 现代地质,17(4);428~434.
- 张旗,王焰,钱青,杨进辉,王元龙,赵太平,郭光军.2001.中国东部燕山期埃达克岩的特征及其构造一成矿意义.岩石学报,17 (2):236~244.
- 张玉清.2009.内蒙古苏尼特左旗巴音乌拉二叠纪埃达克质花岗闪长 岩类地球化学特征及其地质意义. 岩石矿物学杂志,28(4):329 ~338.
- 赵英利,李伟民,温泉波,梁探岳,冯志强,周建平,申亮. 2016. 内蒙东部晚古生代构造格局:来自中、晚二叠一早三叠世砂岩碎屑锆石 U-Pb 年代学的证据. 岩石学报,32(9):2807~2822.
- Atherton M P, Petford N. 1993. Generation of sodium-rich magmas from newly underplated basaltic crust. Nature, 362: 144~146.
- Bao Zhiwei, Chen Senhuang, Zhang Zhentang. 1993 & Study on REE and Sm-Nd isotopes of Hegenshan ophiolite, Inner Mongolia. Chemical, 23(4):339~349.
- Blichert-Toft J, Albarède F. 1997. The Lu-Hf isotope geochemistry of chondrites and the evolution of the mantle-crust system. Earth and Planetary Science Letters, 148:243~258.
- Cao Congzhou, Yang Fanglin, Tian Changlie, Yuan Chao. 1986&. The ophiolite in Hegenshan district, Nei Mongol and the position of suture line hetween Sino—Korean and Siberian plate. In: Contributions to the Project of Pate Tectonics in Northern China (1). Beijing: Geological Publishing House: 64~86.
- Chen Bin, Zhao Guochun, Wilde S. 2001&. Subduction- and collision-related granitoids from southern Sonidzuoqi, Inner Mongolia; isotopic ages and tectonic implications. Geological Review, 47 (4): $361 \sim 367$.
- Defant M J, Drummond M S. 1990. Derivation of some modern arc magmas by melting of young subducted lithosphere. Nature, 347: 662.
- Gao Xiaofeng, Guo Feng, Xiao Peixi, Kang Lei, Xi Rengang. 2016. Geochemical and Sr—Nd—Pb isotopic evidence for ancient lower continental crust beneath the Xi Ujimqin area of NE China. Lithos, 252;173~184.
- Griffin W L, Wang Xiang, Jackson S E, Pearson N J, O'Reilly S Y, Xu

Xisheng, Zhou Xinmin. 2002. Zircon chemistry and magma mixing, SE China: In-situ analysis of Hf isotopes, Tonglu and Pingtan igneous complexes. Lithos, 61:237~269.

263

- He Zhengjun, Liu Shuwen, Ren Jishun, Wang Yu. 1997&. Later Permian—Early Trissic sedimentary evolution and tectonic setting of Linxi region Inner Mongolia. Regional Geology of China, 16(4):403 ~409.
- Hong Dawei, Huang Huaizeng, Xiao Yijun, Xu Haiming, Jin Manyuan. 1994& the permian alkaline granites in central innner mongolia and their geological siganificance. Acta Geologica Sinaca, 68(3):219~ 230.
- Hou Kejun, Li Yanhe, Zou Tianren, Qu Xiaoming, Shi Yuruo and Xie Guiqing. 2007&. Laser ablation-MC-ICP-MS technique for Hf isotope microanalysis of zircon and its geological applications. Acta Petrologica Sinica, 23 (10): 2595~2604.
- Jian Ping, Liu Dunyi, Kröner A, Windley B F, Shi Yuruo, Zhang Wei, Zhang Fuqin, Miao Laicheng, Zhang Liqiao, Tomurhuu D. 2010. Evolution of a Permian intraoceanic arc—trench system in the Solonker suture zone, Central Asian Orogenic Belt, China and Mongolia. Lithos, 118(1~2):169~190.
- Kang Jianli, Xiao Zhibin, Wang Huichu, Chu Hang, Ren Yunwei, Liu Huan, Gao Zhirui, Sun Yiwei. 2016 & Late Paleozoic subduction of the paleo-Asian ocean; geochronological and geochemical evidence from the meta-basic volcanics of Xilinhot, Inner Mongolia. Acta Geologica Sinaca, 90(2):383~397.
- Li Chengdong, Zhang Fuqin, Miao Laicheng, Xie Hangqiang, Xu Yawen. 2007 & Zircon SHRIMP geochronology and geochemistry of Late Permian high-Mg andesites in Seluohe area, Jilin province, China. Acta Petrologica Sinica, 23(4):767~776.
- Li Jinyi, Gao Liming, Sun Guihua, Li Yaping and Wang Yanbin. 2007&. Shuangjingzi Middle Triassic syn-collisional crust-derived granite in the east Inner Mongoloia and its constraint on the timing of collision between Siberian and Sino—Korean paleo-plates. Acta Petrologica Sinica, 23 (3):565~582.
- Li Jinyi, Zhang Jin, Yang Tiannan, Li Yaping, Sun Guihua, Zhu Zhixin, Wang Lijia. 2009&. Crustal tectonic division and evolution of the southern part of the North Asian Orogenic region and its adjacent areas. Journal of Jilin University (Earth Science Edition), 39(4):584~605.
- Li Yingjie, Wang Jinfang, Wang Genhou, Li Hongyang and Dong Peipei. 2018&. Discovery and significance of the Dahate fore-arc basalts from Diyanmiao ophiolite in Inner Mongolia. Acta Petrologica Sinica, 34(2):469~482.
- Li Shuanglin, Quyang Ziyuan.1998 & Tectonic framework and evolution of Xing'an—Mongolian orogenic belt and its adjancent region. Marine Geology & Quaternary Geology, 18(3):46~55.
- Liu Dunyi, Jian Ping, Zhang Qi, Zhang Fuqin, Shi Yuruo, Shi Guanghai, Zhang Nuqiao, Tao Hua. SHRIMP Dating of Adakites in the Tulingkai Ophiolite, Inner Mongolia: Evidence for the Early Paleozoic Subduction. Acta Geologica Sinaca, 77 (3):317~327.
- Liu Jianfeng, Chi Xiaoguo, Zhang Xingzhou, Ma Zhihong, Zhao Zhi, Wang Tiefu, Hu Zhaochu, Zhao Xiuyu. 2009 & Geochemical characteristic of Carboniferous quartz-diorite in the Southern Xiwuqi area, Inner Mongolia and its tectonic significance. Acta Geologica Sinaca, 83 (3):365~376.
- Liu Jianfeng, Li Jinyi, Chi Xiaoguo, Qu Junfeng, Chen Junqiang, Hu Zhaochu, Feng Qianwen. 2016. The tectonic setting of early Permian bimodal volcanism in central Inner Mongolia; continental rift, post-

- collisional extension, or active continental margin? International Geology Review, 58(6):737~755.
- Liu Yongsheng, Gao Shan, Hu Zhaochu, Gao Changgui, Zong Keqing and Wang Dongbing. 2010. Continental and oceanic crust recycling-induced melt—peridotite interactions in the Trans-North China Orogen: U-Pb dating, Hf isotopes and trace elements in zircons from mantle xenoliths. Journal of Petrology, 51(1~2):537~57.
- Liu Jianfeng, Li Jinyi, Chi Xiaoguo, Qu Junfeng, Hu Zhaochu, Guo Chunli. 2014&. Petrological and geochemical characteristics of the Early Triassic granite belt in Southeastern Inner Mongolia and its tectonic setting. Acta Geologica Sinaca, 88 (9):1677~1690.
- Luo Hongling, Wu Tairan and Li Yi. 2007 & Geochemistry and SHRIMP dating of the Kebu massif from Wulatezhongqi, Inner Mongolia: evidence for the Early Permian underplating beneath the North China Craton. Acta Petrologica Sinica, 23(4):755~766.
- Lü Hongbo, Feng Xuedong, Wang Jun, Zhu Xiaoqing, Dong Xiaopeng, Zhang Haichun, Zhang Yuxu. 2018 & Ophiolitic Mélanges found in mount Langshan as the crucial evidence of collisional margin between North China Craton and Central Asian Orogenic Belt. Geological Review, 64(4):777~805.
- Maniar P D, Piccoli P M. 1989. Tectonic discrimination of granitoids. GSA Bull., 101: 635~643.
- Miao Laicheng, Zhang Fuqin, Fan Weiming, Liu Dunyi. 2007.
 Phanerozoic evolution of the Inner Mongolia—Daxing anling orogenic belt in North China: constraints from geochronology of ophiolites and associated formations. Geological Society, London, Special Publications, 280(1):223~237.
- Middlemost E A. 1975. The basalt clan. Earth-Science Reviews, 11(4): $337 \sim 364$.
- Middlemost E A K.1994. Naming materials in the magma/igneous rock system. Earth-Science Reviews, 37(3):215~224.
- Miyashiro A. 1974. Volcanic rock series in island arcs and active continental margins. American Journal of Science, 274; 321~355.
- Peacock S M, Rushmer T, Thompson A B. 1994. Partial melting of subducting oceanic crust. Earth and Planetary Science Letters, 121 (1):227~244.
- Pearce J A, Harris N B W, Tindle A G. 1984. Trace element discrimination diagrams for the tectonic interpretation of granitic rocks. Journal of Petrology, 25(4):956~983.
- Pei Xianzhi, Wang Tao, Ding Saping, Li Yong, Hu Bo. 2003&. Geochemical characteristics and geological significance of Neoproterozoic adaktic granitoids on the north side of the Shangdan zone in the East Qinling. Geology in China, 30(4):372~381.
- Petford N, Michael A.1996. Na-rich Partial melts from newly underplated basaltic crust: the Cordillera Blanca batholith, Peru. Journal of Petrology, 37(6):1491~1521.
- Qin Ya, Liang Yihong, Xing Jilin, Zhang Qingwei, Liu Chengxian. 2013 &.

 The identification of Early Paleozoic type adaktic rocks in Zhengxiangbaiqi area, Inner Mongolia and its significance. Earth Science Frontiers, 20(5):106~114.
- Rapp R P, Shimizu N, Norman M D, Applegate G S. 1999. Reaction between slab-derived melts and peridotite in the mantle wedge: experimental constraints at 3.8 GPa. Chemical Geology, 160(4): 335~356.
- Scherer E, Munker C, Mezger K. 2001. Calibration of the lutetium hafnium clock. Science, 293(5530):683~687.
- Sen C, Dunn T. 1994. Dehydration melting of a basaltic composition amphibolite at 1.5 and 2.0 GPa; implications for the origin of

adakites. Contributions to Mineralogy and Petrology, 117(4):394~409

2019年

- Şengör A M C, Natalin B A, Burtman V S.1993. Evolution of the Altaid tectonic collage and Palaeozoic crustal growth in Eurasia. Nature, 364:299~307.
- Shi Yuruo, Liu Cui, Deng Jinfu and Jian Ping. 2014&. Geochronological frame of granitoids from Central Inner Mongolia and its tectonomagmatic evolution. Acta Petrologica Sinica, 30(11): 3155 ~3171.
- Sun Deyou, Wu Fuyuan, Zhang Yanbin, Gao Shan. 2004&. The final closing time of the west Lamulun River— Changchun— Yanji plate suture zone—Evidence from the Dayushan granitic pluton, Jilin Province. Journal of Jilin University (Earth Science Edition), 34 (2):174~181.
- Sun S S, McDonough W F. 1989. Chemical and isotopic systematics of oceanic basalts; implications for mantle composition and processes. Geological Society, London, Special Publications, 42(1):313 ~ 345.
- Tao Jixiong, Xu Liquan, He Feng, Su Maorong. 2005&. Petrological evidence for subduction of the Early Paleozoic oceanic crust in Bart-Obo, Inner Mongolia. Geological Survey and Reseach, 28 (1):1~ 8.
- Wang Jinfang, Li Yingjie, Li Hongjie, Dong Peipei. 2017 & Discovery of Early Permian intra-oceanic arc adakite in the Meilaotewula Ophiolite, Inner Mongolia and its evolution model. Acta Geologica Sinica, 91 (8):1776~1795.
- Wang Limin, Chi Xiaoguo, Zhao Zhi, Sun Wei, Zhang Rui, Pan Shiyu, Quan Jingyu. 2014. Zircon U-Pb geochronology and geochemistry of the Maoliger quartz monzodiorites, Inner Mongolia, China; implications for Carboniferous arc magmatism and closure of the Palaeo-Asian Ocean. International Geology Review, 56(12):1435~1449
- Wang Qiang, Zhao Zhenhua, Xiong Xialin, Xu Jifeng.2001 & Melting of the underplated basaltic lower crust; Evidence from the Shaxi adakitic sodic quartz diorite-porphyrites, Anhui Province, China. Geochimica, 30 (4):353~362.
- Wang Quan. 1986&. Recognition of the suture between the Sino—Korean and Siberian Paleoplates in the middle part of Inner Mongolian. Acta Geologica Sinica, (1):31~43.
- Wang Quan, Liu Xueya, Li Jinyi. 1991#. Paleoplates tectonics in Inner Mongolian of China. Bullertin of the Chinese Academy of Geological Sciences, (1):1~15.
- Wang Xiang. 2018 . Analysis on the Oreforming Time and Genesis of the Bayan Obo REE—Nb—Fe Deposit; With a Discussion on the Mass Extinction at the P—T Boundary and "AMH Orogeny". Geological Review, 64(2):299~345.
- Wang Yujing, Fan Zhiyong. 1997 & Discovery of Permian radiolarians in ophiolite belt on northern side of Xar Moron River, Inner Monggol and its geological significance. Acta Palaeontologica Sinica, 36(1): 58~69.
- Wood D A. 1980. The application of a Th—Hf—Ta diagram to problems of tectonomagmatic classification and to establishing the nature of crustal contamination of basaltic lavas of the British Tertiary Volcanic Province. Earth and Planetary Science Letters, 50(1):11~30.
- Wu Fuyuan, Sun Deyou, Lin Qiang. 1999 & Petrogenesis of the Phanerozoic granites and crustal growth in Northeast China. Acta Petrologica Sinica, 15(2): 181~189.
- Xiao Wenjiao, Windley B F, Hao Jie, Zhai Mingguo. 2003. Accretion

- leading to collision and the Permian Solonker suture, Inner Mongolia, China; termination of the Central Asian Orogenic Belt. Tectonics, 22(6); 1069; doi:10.1029/2002TC001484
- Xiao Wenjiao, Shu Liangshu, Gao Jun, Xiong Xiaolin, Wang Jingbin, Guo Zhaojie, Li Jinyi, Sun Min. 2008&. Continental dynamics of the central Asian orogenic belt and its metallogeny. Xinjiang Geology, 26 (1):4~8.
- Xiao W J, Windley B F, Huang B C, Han C M, Yuan C, Chen H L, Sun M, Sun S, Li J L. 2009. End-Permian to mid-Triassic termination of the accretionary processes of the southern Altaids: implications for the geodynamic evolution, Phanerozoic continental growth, and metallogeny of Central Asia. International Journal of Earth Sciences, 98(6):1189~1217.
- Xu Bei, Chen Bin. 1993. The opposite subduction and collision between the Siberian and Sino—Korean plates during the Early—Middle Paleozoic. Report No. 4 of the IGCP Project 283: Geodynamic Evolution Paleoasian Ocean. Novosibirsk, Russia: 148~150.
- Xu Bei, Zhao Pan, Bao Qingzhong, Zhou Yongheng, Wang Yanyang, Luo Zhiwen. 2014&. Preliminary study on the pre-Mesozoic tectonic unit division of the Xing—Meng Orogenic Belt (XMOB). Acta Petrologica Sinica, 30 (7): 1841~1857.
- Xu Jifeng, Wu Jianbin, Wang Qian, Chen Jianlin, Cao Kang. 2014&.
 Research advances of adakites and adakitic rocks in China. Bulletin of Mineralogy, Petrology and Geochemistry, 33 (1):6~13.
- Xu Liquan, Deng Jinfu, Chen Zhiyong, Tao Jixiong. 2003&. The identification of Ordovician adakites and its signification in northern Damao, Inner Mongolia. Geoscience, 17 (4):428~434.
- Yang Jinhui, Wu Fuyuan, Shao Jian, Wilde S A, Xie Liewen, Liu

- Xiaoming. 2006. Constraints on the timing of uplift of the Yanshan Fold and Thrust Belt, North China. Earth and Planetary Science Letters, 246(3):336~352.
- Yu Shengyao, Zhang Jianxin, Qin Haipeng, Sun Deyou, Zhao Xilin, Cong Feng, Li Yunshuai. 2015. Petrogenesis of the Early Paleozoic low-Mg and high-Mg adakitic rocks in the North Qilian orogenic belt, NW China: Implications for transition from crustal thickening to extension thinning. Journal of Asian Earth Sciences, 107: 122~ 139.
- Zhang Qi, Wang Yan, Qian Qing, Yang Jinhui, Wang Yuanlong, Zhao Taiping and Guo Guangjun. 2001&. The characteristics and tectonic—metallogenic significances of the adakites in Yanshanian period from eastern China. Acta Petrologica Sinica, 17(2): 236~244
- Zhang Xiaohui, Zhang Hongfu, Tang Yanjie, Wilde S A, Hu Zhaochu. 2008. Geochemistry of Permian bimodal volcanic rocks from central Inner Mongolia, North China: Implication for tectonic setting and Phanerozoic continental growth in Central Asian Orogenic Belt. Chemical Geology, 249 (3~4):262~281.
- Zhang Yuqing. 2009 &. Geochemical characteristics of Permian adakitic granodiorite in Bayinwula of Sonid Left Banner, Inner Mongolia. Acta Petrologica et Mineralgica, 28 (4):329~338.
- Zhao Yingli, Li Weimin, Wen Quanbo, Liang Chenyue, Feng Zhiqiang, Zhou Jianping and Shen Liang. 2016 & Late Paleozoic tectonic framework of eastern Inner Mongolia: Evidence from the detrital zircon U-Pb ages of the Mid—late Permian to Early Triassic sandstones. Acta Petrologica Sinica, 32(9):2807~2822.

Zircon U-Pb Ages, Geochemical Characteristics of Late Permian Granite in West Ujimqin Banner, Inner Mongolia, and Tectonic Significance

FAN Yuxu¹⁾, LI Tingdong¹⁾, XIAO Qinghui¹⁾, CHENG Yang²⁾, LI Yan²⁾, GUO Lingjun³⁾, LUO Pengyue³⁾

- 1) Institute of Geology, Chinese academy of Geological Sciences, Beijing, 100037;
- 2) Institute of Mineral Resources, China Metallurgical Geology Administration, Beijing, 101300;
 - 3) Geological Survey Institute of Inner Mongolia, Hohhot, 010020

Objectives: Adakite is a kind of intermediate—acid rock with unique geochemical characteristics. It can track the oceanic crust subduction and crustal thickening and other related events in geological history, which is of great significance for the inversion of crustal composition and mineralization. According to previous studies, the granites of Seerbeng and Nuhetingshala in West Ujimqin have the characteristics of adakite, but lacked accurate chronology data. The study on the diagenetic age and tectonic background of the adakite granitoids is helpful to understand the tectonic evolution of the paleo- Asian Ocean.

Methods: Based on the field work, through the microscope observation, the whole rock chemical analysis, LA-ICP-MS U-Pb zircon dating of the granitiods and the Hf isotopic analysis.

Results: The U-Pb isotopic dating of zircon shows that the ages of Seerbeng pluton and Nuhetingshala pluton in West Ujimqin area are 255.3 ± 0.7 Ma and 254.4 ± 1.2 Ma, which are the products of magmatic activity in the late Permian. By lithology and rock geochemistry analysis found that belong to calc-alkalic rock and high potassium calcalkali series, SiO_2 content is $65\% \sim 73\%$, Na-rich and K-poor, high Sr, low Yb Y and high Sr/Y, wich consistent with the characteristics of typical adakite. The magmatic zircons are positively $\varepsilon Hf(t)$ values (+8.1 \sim +13.3) and young two-stage model ages varied in $430 \sim 760 Ma$. Adakite rock formation is related to partial melting of young

subduction plate, and the high Mg# indicates that magmatic melts interact with mantle peridotite.

Conclusions: Combined with regional rock assemblages, the paleo-Asian Ocean has not yet completely closed in late Permian. During this stage, the subducted oceanic crust broke off and partially melted, which formed the adakite granitoids and hight-Mg andesite. The closing time of the paleo-Asian ocean should be after the Permian.

Keywords: Late Permian; high-Sr low-Yb granitoids (Adakite); U-Pb age of zircon; tectonic setting; Inner Mongolia

Acknowledgements: This study is support by Geological Mineral Exploration Projects of Inner Mongolia (No. 2017-YS01), China Geological Survey Project (No. DD20160345).

First author: FAN Yuxu, male, born in 1987, Ph.D candidate. Email: 562442919@ qq.com

Corresponding author: XIAO Qinghui, male, born in 1939, engaged in geotectonics of granite, metallogenic geological background of mineral resources and three-dimensional structure of lithosphere in China. Email: qinghuixiao@ 126.com

Manuscript received on: 2018-06-13; Accepted on: 2018-10-13; Edited by: ZHANG Yuxu **Doi**: 10.16509/j.georeview.2019.01.017

GEOLOGICAL REVIEW

Vol. 65 No. 1 2019

CONTENTS

Writting Papers in Chinese, to Benefit Chinese People First——New Year's Message in 2019 from the 40th Committee of Geological Review YANG Wencai, ZHANG Yuxu (1)
Scholarly Discussion
Crustal P-wave Seismic Tomography of the Qinghai—Xizang (Tibetan) Plateau ·····
Ring Structure of Northern Pishan in the Southern Xinjiang: Record from Meteorite Impact
Discussing on the Duplication of O m in the Well Zhenjia-1 Northern Shaanxi Salt Depression, Ordos Basin
Weathering Characteristics of the Surface Sediments and Their Indications for Biological Process in the Liaohe Delta Wetlands
LI Tongtong, YE Siyuan, HAN Zongzhu, YUAN Hongming, PEI Lixin(50)
The Petrogenesis and Tectonic Setting of the Keratophye in the Dayimalong Area of the Northern Qilian Orogenic Belt
BU Tao, WANG Guoqiang, TANG Zhuo, ZHU Tao, LUO Gengen, JI Bo (63)
Identification of the Permian E-MORBType Basalts and Their Tectonic Significance from Shiyan Area, Wudang Mountain
Deformational Characteristics and LA-ICP-MS Zircon U-Pb Ages of Granites at Shiershan in the Jiangnan Orogen and Their
Geological Significance
Geological Significance
U-Pb Geochronology of Zircons from the Volcanic Rocks in Bingounan Formation, Southern Altyn Tagh: Implication for
the Precambrian ·····
··· ZENG Zhongcheng, BIAN Xiaowei, ZHAO Jianglin, LIU Xiangdong, ZHANG Ruoyu, LI Qi, HE Yuanfang, JIAN Kunkun(117)
LA-ICP-MS Zircon U-Pb Ages, Geochemical Characteristics of the Dashizhai Formation Tuffs in Hexigten Banner, Inner Mongolia
and Thier Tectonic Significance